UNIVERSITY OF MINES AND TECHNOLOGY
TARKWA

FACULTY OF MINERAL RESOURCES TECHNOLOGY

DEPARTMENT OF MINERALS ENGINEERING

A THESIS REPORT ENTITLED

NATURE OF THE OPON MANSI IRON ORE AND ITS RESPONSE TO REDUCTION BY END-OF-LIFE VEHICLE TYRES.

BY

CHRISTOPH YAO BADU

SUBMITTED IN FULFILMENT OF THE REQUIREMENTS FOR THE AWARD OF MASTER OF PHILOSOPHY DEGREE IN MINERALS ENGINEERING

THESIS SUPERVISOR

.....

ASSOC PROF JAMES RANSFORD DANKWAH

TARKWA, GHANA

SEPTEMBER, 2021

DECLARATION

I declare that this thesis work is my own work. It is being submitted for the degree of Master of Philosophy in Minerals Engineering in the University of Mines and Technology (UMaT), Tarkwa. It has not been submitted for any degree or examination in any other University.

…….

(Signature of Candidate)

…….. day of September, 2021.

ABSTRACT

The nature of Opon Mansi iron ore and its ability to be reduced by the carbonaceous material generated from end-of-life vehicle tyre (ELT) was investigated in this work. Pulverised samples of the ores were subjected to X-ray fluorescence (XRF), X-ray diffraction (XRD) and Scanning Electron Microscopy-Energy Dispersive Spectroscopy (SEM/EDS) analysis to characterize the ore. XRF, XRD and SEM-EDS analysis revealed that the Opon Mansi iron ore used in the studies was a low grade hematite iron ore with 41.07% Fe_2O_3 (28.75% Fe), with the presence of gangue minerals (19% Al_2O_3 and 24.97% SiO_2) and deleterious elements (0.03% sulfur and 0.05% phosphorous). Pudo non-magnetic ore because of its fluxing materials (MgO and CaO) was blended with with the Opon Mansi iron ore to improve on the extent of reduction. Carbonaceous material was obtained from ELTs by pulverising charred ELTs. Reduction studies was conducted on composite pellets formed from mixture of the iron ore containing charred ELT and binder in a domestic microwave oven and the extent of reduction was calculated after microwave irradiation for 20, 30, 40, 50 and 60 minutes. The extent of reduction at 60 minutes was 94.49%. Gas reduction studies was also conducted on the pellets in a horizontal resistance tube furnace to study the amount of gases that were evolved in the reduction of the ore. The extent of reduction was also calculated from amount of gases that were evolved. XRF, XRD and SEM-EDS analysis was conducted on the reduced iron ore and ELT composite pellet. Hematite was completely reduced to metal iron at 60 minutes. The reducted metal contained 75% Fe which indicates that ELT is a potential replacement for metallurgical coke.

DEDICATION

This thesis is dedicated to my wife,

Mrs Katherine Ama Dorcas Mununkum Badu for her relentless support throughout my study.

ACKNOWLEDGEMENTS

I give my Father in Heaven all the glory and thanks for the grace and wisdom given me to put this thesis work together. God, I also thank you for the help, insight, direction and good health you provided me to finish this work.

I am grateful to supervisor Prof. James Ransford Dankwah for his enormous contributions and support to my work.

I would like to thank all the staff of the department of the minerals engineering of UMaT for their friendly advice and motivation to carry on the research.

I would like to thank all those who have contributed in different ways to make this work a success.

TABLE OF CONTENT

LIST OF FIGURES

LIST OF TABLES

CHAPTER 1
INTRODUCTION

1.1 Statement of Problem

Opon Mansi is in the Western Region of Ghana. It has iron ore deposits that are located on top of the range of fifteen hills which extend over a distance of 24 km from Opon-Valley (Timbillah, et al., 2007). This iron ore can be exploited if the raw material (including reducing agents) is available. Coking coal and metallurgical coke are the main reductants used in iron and steelmaking processes (Suopajärvi *et al.*, 2017).

However, this conventional material is not readily available in Ghana and therefore must be imported at a high cost. Rubber tyre is an elastomer consisting of the co-polymers styrene and butadiene and is a rich source of carbon - and hydrogen (Dankwah *et al.*, 2012; Dankwah and Koshy, 2013). It can be a replacement for metallurgical coke. One of the main source of waste in End-of-Life vehicles (ELVs) is End-of-Life Tyres (ELTs). Globally, about 1.5 billion units of tyres are estimated to be produced a year and almost the same quantity falls into the category of ELTs (Landi, et al., 2016). Most of these ELTs are export to undeveloped and underdeveloped countries (where Ghana is classified) as home used tires. Due to their physicochemical properties, the vulcanized rubber fraction of used tyres represents a challenge for the solid waste industry. The most common rubbers used in the manufacture of tyres are cis-polybutadiene rubber (CBR), isobutylene-isoprene copolymer rubber (i.e., butyl rubber (BR)) and styrene-butadiene copolymer rubber (Ramirez-Canon, et al., 2018). This poses a threat as rodents and disease-carrying insects like mosquitoes hide in them. Stockpiles of ELTs can be a fire hazard through lightning strikes or arsonists.

The aim of this research is therefore to investigate the use of ELTs as a potential replacement for metallurgical coke in the production of metallic iron from the Opon Mansi iron ore and the nature of the ore.

1.2 Research Objectives

The objective of this research is to investigate;

i. The nature of the Opon Mansi iron ore.
ii. The viability of using end-of-Life vehicle tyre to replace metallurgical coke.

1.3 Methods and Procedures Used

The methods and procedures used for this research included:

a. Review of relevant literature on the field of study
b. Experimental work
    i. Field collection of ore sample;
    ii. Sample preparation;
    iii. X-ray fluorescence analysis (XRF)
    iv. X-Ray Diffraction analysis (XRD)
    v. Scanning electron microscope analysis (SEM)
    vi. Reduction studies.
c. Analysis of the results
d. Report writing

1.4 Facilities used

The facilities used for this thesis included:

a. Minerals Engineering Laboratory, University of Mines and Technology;
b. University of Mines and Technology library; and
c. Analytical Centre, School of Chemical Science and Engineering, UNSW, Sydney, Australia.

1.5 Chapter Outline

The chapter outline for this research report is as follows;

i. Chapter 1 Introduction. It will talk about the research topic
ii. Chapter 2 Literature review. It will talk about the characteristics of iron ore that was used to determine the nature of the ore. It elucidates the kinetics of iron reduction and the reactions involved.

iii. Chapter 3 Materials and Methods. In this chapter, the materials and methods that were employed during the experiment will be highlighted.

iv. Chapter 4 Results and Discussion. This chapter discusses the results obtained from the experiment and laboratory analysis conducted.

v. Chapter 5 Conclusion and Recommendations

CHAPTER 2
LITERATURE REVIEW

2.1 Iron Ore

Iron is among the most abundant elements on earth. But in nature, it does not occur in its pure-metallic form. The term iron ore is applied to any natural iron-bearing mineral or rock in which the content of iron is high enough to be extracted commercially (Taylor *et al.*, 2009). Iron ore is an important raw material for iron and steel industry, and its quality dictates the production strategy, and ultimately, the quality and cost of steel (Kumar *et al.*, 2007). To justify the investment during exploitation, the impurity elements content of iron ores must be low (Kiptarus *et al.*, 2015).

The earth's crust is composed of 5% Iron ore. Hematite, magnetite, limonite and siderite are iron minerals that presently used as ore and occasionally ankerite, goethite and turgite. Hematite is the most important iron ore (Michaud, 2016).

2.1.1 Formation of Iron Ore Deposit

Banded iron formations (BIFs) are chemical marine sediments of Precambrian origin. They contain at least 15 % bulk Fe content and are characterized by spectacular Fe-rich bands alternating with cherty Si-rich layers (Fru *et al.*, 2018). BIF is defined as a sedimentary rock consisting of alternating millimeter to centimeter scale iron-rich and iron-poor bands typically bands of iron oxide and chert, although iron carbonate and iron silicate bands may be important locally. This definition excludes all rocks that have had iron-poor bands removed by post sedimentation processes including all high-grade iron ore (Lascelles, 2012).

The largest iron deposits formed almost exclusively during the Precambrian time even though they are widespread geologically. Iron formation are generally in bands which consist of iron such as siderite, magnetite and hematite with silica in the form chert, jasper etc, but sometimes not distinctly so (Michaud, 2016). The extensive deposits

of banded iron-formation are formed during Neoarchean and Paleoproterozoic and associated with marine sedimentary units (Taylor *et al.*, 2009). The enrichment of Precambrian iron-formations has led most world-class high grade (60-67 wt. percent Fe) hematite iron ore deposits (Smith and Beukes, 2016).

2.1.2 Classification of Iron Ore

In iron ores, the Fe content is lowered according to the amount of impurities present. Overall, the quality of iron ore is mainly classified based on the Fe content. More specifically, ores with Fe contents above 65% are regarded as high-grade ores; 62–64% medium- (or average) grade ores and those below 58% Fe are considered as low-grade ores (Muwanguzi *et al.*, 2012b). According to Palacios, 2011, industrial iron ores (magnetite, hematite, limonite and siderite), high-grade ores contain more than 55 % iron. For an ore to be economically exploitable, its iron contents must be greater than 25% which is referred to as the cut-off grade (Palacios, 2011; Ofoegbu, 2019). Iron ore can be classified by grade as shown in Table 2.1.

Table 2.1 Classes of Iron Ore (Kiptarus et al., 2015)

Component	Total Iron Content		
	Low	Medium	High
Content Mass %	>56	62-64	>64

2.1.3 Types of Iron Minerals in Iron Ore

The most commonly used iron-bearing minerals contain iron compounds as follows: hematite, Fe_2O_3 (70% Fe); magnetite, Fe_3O_4 (72.4% Fe) and of much less importance are: limonite, $2Fe_2O_3 \cdot 3H_2O$ (60% Fe); siderite, $FeCO_3$ (48.3% Fe); pyrite, FeS_2 (46.6% Fe) (Muwanguzi *et al.*, 2012b).

Hematite ore (Fe_2O_3) is a natural ore with naturally high iron content of 70% Fe. Because of its high iron content, hematite ore must undergo only a simple crushing, screening and blending process before being shipped off for steel production. Natural ores typically have iron (Fe) content of between 56% Fe and 64% Fe when mined

(Kay, 2018). Hematite deposits are mostly sedimentary in origin, such as the BIFs (Harry et al., 1973). Hematite possesses a higher ratio of oxygen (O/Fe = 1.5) than magnetite (O/Fe = 1.33), but hematite is easily reducible than magnetite because magnetite is crystalline. This makes magnetite less reactive and displays a lower ability to reduce than hematite (Palacios, 2011).

Magnetite (Fe_3O_4) actually has higher iron content (72% Fe) than the mineral hematite (70% Fe). However, while hematite ore generally contains large concentrations of hematite, magnetite ore generally holds low concentrations of magnetite. As a result, this type of iron ore must be concentrated before it can be used to produce steel. Magnetite ore's magnetic properties are helpful during this process (Kay, 2018). High grade magnetite ore normally contains more than 60% iron with some impurities such as silica, alumina and phosphorus. Magnetite is beneficiated by crushing and then separating the magnetite from the gangue minerals with a magnet. This separation is usually so efficient that a lower grade magnetite ore can be treated easily than a comparable grade of hematite ore (Amikiya, 2014).

Goethite, α-FeO(OH), is one of the most widespread forms of iron oxides in terrestrial soils, sediments and ore deposits, as well as a common weathering product in rocks of all types. It transforms to hematite (α-Fe_2O_3) between 453 and 543 K through dehydrogenation and has been used extensively in the preparation of maghemite (α-Fe_2O_3) in magnetic storage media. The crystal structure of goethite was first determined by Goldsztaub (1935) and Hoppe (1940) using X-ray diffraction photographic techniques (Yang *et al.*, 2006).

Limonite (FeO(OH)) usually occurs as a secondary material, formed from the weathering of hematite, magnetite, pyrite, and other iron-bearing materials. Limonite is often stalactitic, reniform, botryoidal, or mammillary in habit, rather than crystalline. It also occurs as pseudomorphs and coatings on the walls of fractures and cavities. Researchers who studied "limonite" discovered that it is amorphous and has a variable composition. It often contains significant amounts of iron oxide minerals such as

goethite and hematite. This research revealed that the material called "limonite" does not meet the definition of a mineral. Instead, limonite is a mineraloid composed mainly of hydrous iron oxides that are often found in intimate associations with iron minerals (King, 2020).

Siderite ($FeCO_3$) is a mineral which derives its name from the word sideros, meaning iron in Greek. Siderite minerals contains about 48.02% iron (Fe) and is a crystal trigonal (hexagonal scalenohedral) system, mostly rhombohedral crystalline; plate, prismatic, massive; medium-fine grained; rarely kidney, oolitic crystal habits. Siderite minerals have transparent-semi-transparent appearance and have different colours like yellowish-brown to greyish-brown, pale yellow to tannish, grey, brown, green, red, black and sometimes nearly colourless; tarnished iridescent at times; colourless to yellow and yellow-brown in transmitted light. The specific weight of siderite mineral is 3.96 g/cm3 and its Mohs hardness is between 3.5 and 4.5 (Celikdemir *et al.*, 2018).

2.1.4 Gangue Minerals Associated and its Effects

According to Fathi Habashi, impurities in iron ore plays an important role in the blast furnace because they influence the quality of the product and the life of refractory lining. The behavior of impurities varies considerably and can be divided as follows;

Unobjectionable Impurities

They are impurities which are not reduced, eg. Al_2O_3 and MgO. They are also valuable fluxes (Habashi, 1997). A small increase in the alumina content of sinter blends can have a significant adverse impact on the strength and reduction degradation characteristics of final sinter, leading to deterioration in gas permeability in the upper part of the blast furnace. It could also alter the composition and properties of the primary melt formed in sinter located near the cohesive zone of the blast furnace, which would have a negative impact on the gas and liquid permeability and reducibility of sinter in the lower part of the blast furnace. Finally, it increases the alumina loading into the blast furnace and therefore the furnace slag volume, leading to increased coke consumption (Lu, Holmes and Manuel, 2007).

Impurities that Completely Enter the Pig Iron

These are phosphorus, copper, tin, nickel, and vanadium. The reduction of the compounds of these elements take place readily. Of these the most serious is phosphorus since it has to be completely removed to make an acceptable steel (Habashi, 1997). According to Muwanguzi *et al.*, 2012, Phosphorus in steel makes it brittle. More specifically, phosphorus lowers the solidification temperature, increases fluidity, and renders the metal very fluid indirectly through the production of a low melting constituent in iron and steel making. Moreover, phosphorus increases the cold shortness of steel. Unfortunately, phosphorus cannot be effectively removed from iron ores by fluxing and smelting during preparation of raw materials for the blast furnace process (Michaud, 2016).

Impurities that Partially Enter the Pig Iron

These are manganese, silicon, titanium, and Sulphur (Habashi, 1997). Sulphur in the ore goes partly into the iron and steel and makes them brittle (Michaud, 2016). Small amounts of sulphur in iron also have significant deleterious effects on the final properties of products (such as red and hot shortness). Here, Sulphur can exist as either iron sulfide (FeS), which tends to promote cementite producing a harder iron, or as manganese sulfide (MnS), which hardens the iron. The content of S in ores can be decreased by roasting and washing during preparation of raw materials to be used in the blast furnace process (Muwanguzi *et al.*, 2012b). The reduction of MnO_2, SiO_2, and TiO_2 takes place only at high temperatures, therefore, the presence of the respective metals in pig iron will be a function of temperature in the hearth; usually about 70% of these metals enter the pig iron. Titanium is especially undesirable because its presence in the slag, even in small amounts, increase its viscosity. Manganese, silicon, and sulfur must be removed later in the steelmaking process (Habashi, 1997). At present, ores containing more than 5% or 6% of titanic acid (TiO_2) are not saleable (Michaud, 2016). 1% increase in gangue content of the ore results in 1.75% increase in coke rate (Dutta and Chokshi, 2020).

Impurities that Accumulate in the Furnace

These are the alkali metals and zinc. Compounds of these metals are readily reduced (Habashi, 1997).

Gangue minerals are shown as required in blast furnace feed in Table 2.2

Table 2.2 Gangue Content Requirement(Kiptarus *et al.*, 2015; Michaud, 2016)

Component	SiO_2	Al_2O_3	S	P	TiO_2
Content Mass %	3-4	5-6	<0.1	0.05-0.07	<5

2.1.5 Characterisation of Iron Ore

Mineral deposits are considered as naturally occurring substances existing in association with other substances formed due to geochemical processes. The occurrence of most minerals as co-associates with other material requires the characterisation of their compositions to establish understanding of the status of valuable and the unwanted associates (Kolawole *et al.*, 2019). The characterisation of the ores is based on granulometry, texture, mineralogy, physical and chemical properties may aid the mineral processing entrepreneur (Krishna *et al.*, 2013). Characterisation contributes to determination of the iron ores' downstream beneficiation operations and subsequent steelmaking processing, allowing improvements on both new and existing processes (Gomes and Paciornik, 2008).

X-ray fluorescence (XRF), X-ray diffraction (XRD), and scanning electron microscopy (SEM) with energy dispersive X-ray spectrometry (EDS) analyser help to determine the elemental composition, mineral phases which are present, and the morphological conditions of both the ore and reduced product respectively.

2.2 Characterisation Techniques

Qualitative and quantitative methods of analysis are used to characterize samples (Hapugoda, et al., 2009). Optical microscopy, powder X-ray diffraction (PXRD), scanning electron microscopy (SEM), often supplemented with energy-dispersive X-

ray spectroscopy (EDS) and electron-probe microanalysis (EPMA) have represented the key methods used to characterise material properties (Hapugoda, et al., 2009; Hrstka et al., 2018).

2.2.1 X-Ray Diffractometric (XRD) Analysis

X-ray diffraction (XRD) is the key tool in mineral exploration. Mineralogists have been among the foremost in developing and promoting the new field of X-ray crystallography after its discovery. Each mineral type is defined by a characteristic crystal structure, which will give a unique X-ray diffraction pattern, allowing rapid identification of minerals present within a rock or soil sample. The XRD data can be analyzed to determine the proportion of the different minerals present (Bunaciu, et al., 2015).

XRD is a powerful nondestructive technique for characterizing crystalline materials. It provides information on structures, phases, texture, and other structural parameters, such as average grain size, crystallinity, strain, and crystal defects. X-ray diffraction peaks are produced by constructive interference of a monochromatic beam of X-rays scattered at specific angles from each set of lattice planes in a sample. The peak intensities are determined by the distribution of atoms within the lattice. Consequently, the X-ray diffraction pattern is the fingerprint of periodic atomic arrangements in a given material (Bunaciu, et al., 2015).

Most X-ray diffraction techniques rely exclusively on the portion of X-rays elastically scattered by electrons (Thomson scattering). The diffraction event can be visualized as a consequence of the interaction between electromagnetic radiation and electrons. (Lavina, et al., 2014).

X-ray powder diffraction is a crystallographic technique for characterizing structure and phase composition of crystalline samples when the sample is prepared in a polycrystalline form. Powder diffraction is one of the principal research tools of mineralogists, since many minerals are available in polycrystalline form (Lavina, et al., 2014). In powder X-ray diffraction, the diffraction pattern is obtained from a powder

of the material, rather than an individual crystal. Powder diffraction is often easier and more convenient than single crystal diffraction as it does not require individual crystals. A diffraction pattern plots intensity against the angle of the detector, 2θ. The result obtained is called diffractogram (Chauhan and Chauhan, 2014). A typical diffractgram is illustrated in Figure 2.1.

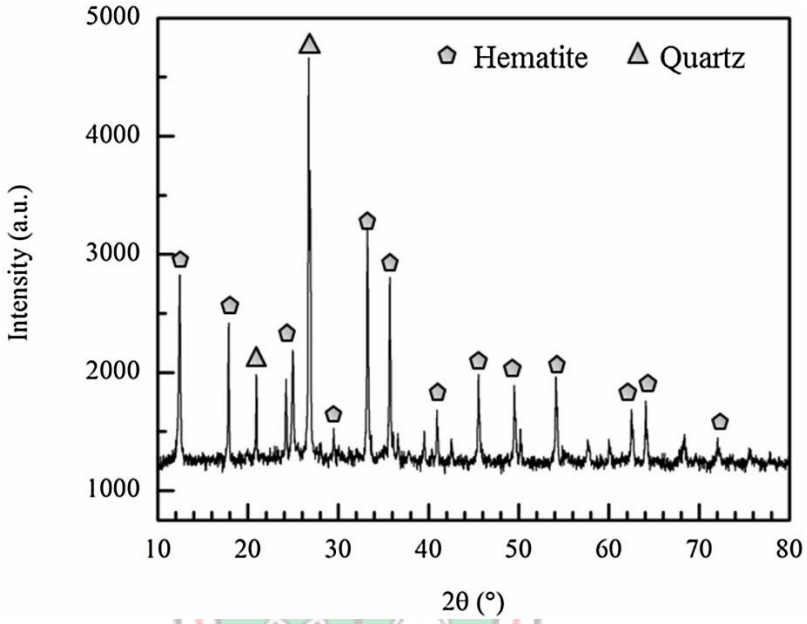

Figure 2.1 An Example of a diffractogram

In a diffraction pattern, the peak position depends upon the wavelength. Absolute intensity (number of X-rays observed in a given peak) may vary by instrumental and experimental parameters (Chauhan and Chauhan, 2014).

2.2.2 X-Ray Fluorescence (XRF) Analysis

X-ray fluorescence is a well-established and powerful tool for nondestructive elemental analysis of virtually any material. It is widely used for environmental, industrial, pharmaceutical, forensic, and scientific research applications to determine the presence or absence and in some cases to measure the concentration of elemental constituents or contaminants (Chen, et al., 2008).

XRF occurs when a fluorescent (or secondary) x-ray is emitted from a sample that is being excited by a primary x-ray source. Because this fluorescence is unique to the

elemental composition of the sample, XRF is an excellent technology for qualitative and quantitative analysis of the material composition (Yerly, 2014).

Although the energy-dispersive (ED) XRF can be used to generate quantitative data if appropriate standard-controlled calibration exists, often it is ideally suited for qualitative elemental analysis since band assignment for the XRF spectrum is easy and each element occurs at a fixed position. XRF can be readily utilised as a quantitative method of elemental composition analysis since the peak height of an element is often related to the concentration in the sample. Quantitative XRF analysis generally uses two main techniques, the Fundamental Parameters Method (FPM) and the calibration with standards method. These two techniques are always incorporated in the XRF instrument software. The FPM is used to calculate the element concentration based on the peak intensities, while the Calibration Standard is used to relate peak intensities to element concentration by deriving calibration curves from materials of known/certified composition (Oyedotun, 2018).

2.2.3 Scanning Electron Microscopy -Energy Dispersive X-Ray Spectroscopy (SEM-EDS) Analysis

In scanning electron microscopy (SEM), a highly energetic and focused electron beam scans the sample and normally provides an extremely enlarged image of the morphology of the sample, as well as information on its chemical composition using an energy dispersive spectrometer (EDS) detector. SEM-EDS is mainly used for characterization of materials, but lately its application has been extended to study organic-based specimens (Girão, et al., 2017).

The sample is shot in a SEM using high-energy electron, and the outcoming electrons/X-rays are analysed. These outcoming electrons/X-rays give information about topography, morphology, composition, orientation of grains, crystallographic information, etc. of a material. Morphology indicates the shape and size, while topography indicates the surface features of an object or "how it looks", its texture, smoothness or roughness. Likewise, composition means elements and compounds that constitute the material, while crystallography means the arrangement of atoms

in the materials. SEM is the leading apparatus that is capable of achieving a detailed visual image of a particle with high-quality and spatial resolution of 1 nm. Although SEM is used just to visualize surface images of a material and does not give any internal information, it is still considered as a powerful instrument that can be used in characterizing crystallographic, magnetic and electrical features of the sample and in determining if any morphological changes of the particle has occurred after modifying the sample surface with other molecules (Akhtar *et al.*, 2018). An example of SEM/EDS of an iron oxide ore is illustrated in Figure 2.2.

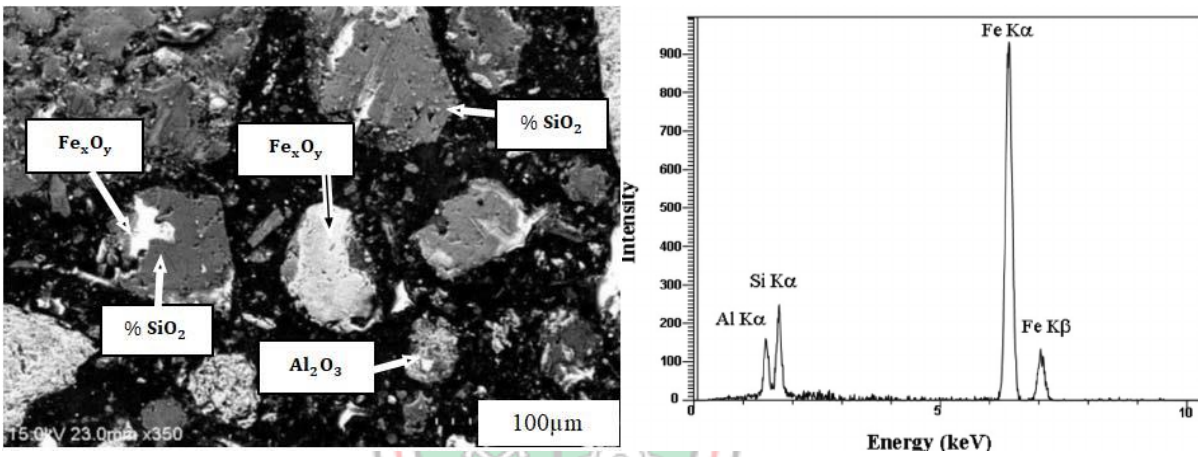

Figure 2.2 SEM and EDS micrograph of an iron ore

2.3 Iron Ore Deposit in Ghana

In Ghana Geological survey has shown that there are abundant iron ore deposits are found in some part of the country. These include the Opon-Mansi iron ore deposit in the Western Region, Sheini iron ore deposit in the Northern Region which is about 1.7 billion metric tons, Pudo iron ore deposit in the Upper West Region, Akpafu iron ore deposit in the Volta Region.

2.3.1 Opon Mansi Iron Ore Deposits

The Opon Mansi iron ore deposits are located on top of the range of fifteen hills which extend over a distance of 24 km from Opon-Valley in the Western Region in the south of Dunkwa, Central Region in the north. The hills on which the iron ores occur have an average height of 400m and the Wuowuo hill, the largest and the highest is 450

m above sea level. The range is in a forest reserve derives its name from its location between two rivers, the Opon and Mansi, both tributaries of the Pra river. The Wuowuo hill, 1 km wide, 2 km in length, stands in prominence in the surrounding country (Timbillah, et al., 2007).

The Opon-Mansi iron ore is a product of lateritization, a process typical of tropical weathering whereby the upper layers of the weathered mantle become enriched with sesquioxides (ratio 2:3 i.e. Mn_2O_3) of elements such as iron, aluminium, manganese while silica, lime, magnesia and the alkalis are generally removed in solution. The end product of lateritization, depending on the parent rock could be Al-rich laterite (Bauxite), Fe-rich laterite such as Opon-Mansi's or Mn-rich laterite such as Nsuta's. The Opon-Mansi ore is an iron-rich laterite. The average chemical composition of Fe_2O_3 is 75.14% with the Fe content ranging 34-45%. Thickness of lateritic ore ranges 9-27m. About 147 million tonnes of ore indicated area 4 square kilometers with Fe content 52.5% (Timbillah, et al., 2007).

The estimated reserves of ore in Wuowuo Hill are large enough to supply the steelwork for period of 18 years (18 million tonnes). On the basis of other close by deposits (80-90 million tonnes), the period could be considerably prolonged (Timbillah, et al., 2007).

2.3.2 Pudo Titaniferous-Magnetite Ore Deposits (Upper-West Region of Ghana)

These iron ore deposits occur in two distinct zones north and south of Pudo, a village in the Tume district in the northeastern part of the Upper West Region. The main magnetite-bearing zone outcrops 1.20 km NW of Pudo and extends for 5.50 km NE (Timbillah, et al., 2007).

2.3.3 Shieni Iron Ore Deposits (Northern Region of Ghana)

The deposits occur almost entirely in the Northern Region about 160 km east of Tamale. The deposits form a N-S range of hills, which rise about 60m above the surrounding plain stretching more than 36 km. The deposits are divided into Northern and Southern groups with a subsidiary group further south. Accessibility to the area

is rather poor but with the development of the Volta Lake, the Oti River draining the area should be navigable to less than 80km from the Shieni deposits. Total estimated reserves 1.270 million metric tonnes (Timbillah, et al., 2007).

2.4 Iron ore Production

Mining (extraction), beneficiation, and processing of iron ore produces iron and steel (Satyendra, 2015). According to Brightmore, global iron ore production in 2019 which was 3,322mnt is estimated to grow to 3,430mnt by 2028. This represent annual mean growth of 0.2%, which is a significant slowdown from a mean growth of 4.5% during 2009-2018. Iron ore is reduced in a blast furnace to produce iron in the form of pig iron which according to fathi Habashi should have a carbon content between 3.5% to 4.25%. Pig iron is the main source of raw material in steel production. From Dankwah *et al.* (2015), iron production in one year exceeds that of all other metals combined in ten years.

2.4.1 Iron Ore Mining

The type of iron ore being mined determines the method by which the ore must be mine. Mining technique involves drilling, blasting, excavation (Okoro *et al.*, 2017). It is often necessary to mine through or remove waste material (also known as overburden) which is not of an interest to gain access to the iron ore deposit within an area. There are two types of mining techniques which are based on excavation methods. These are surface mining and underground mining (Satyendra, 2014b).

Satyendra, 2014a mentioned that iron ore is mostly mined by surface operations. Open pit and open cut mining methods are the most predominant surface mining methods used for mining of iron ores. Open pit and open cast mining accounts for about 96% of non-metal minerals, 87% of metallic ores and 60% of coal production in the world (Amikiya, 2014). However, a few underground iron ore mines are also in operation around the world. The decision for employing surface mining or underground mining depends on the proximity of the ore body to the surface. Open pit and open cut mining are less expensive techniques for ore extraction. Overburden

and stripping ratios are important in determining whether a deposit is to be mined. The stripping ratio describes the unit of waste that must be removed for each unit of unrefined ore mined (Satyendra, 2014b).

2.5 Iron Ore Processing

Iron ore deposit must contain at least 25% iron to be considered economically recoverable. Ores with iron content less than 25% can still be economically exploited if the ore deposit is large, can be concentrated, and can be transported cheaply (Ofoegbu, 2019). Ore processing is the separation of iron ore from gangue to optimize the blast furnace process (Lu, 2015). Iron is recovered from its ore through ore processing (beneficiation and agglomeration) (Singh *et al.*, 2015) then Reduction by blast furnace or DR process (Béchara *et al.*, 2020).

2.5.1 Beneficiation

Most High grade iron ores can be sent directly to iron extraction plants without beneficiation activities except crushing and washing (US EPA, 1994). Low grade iron ores cannot be used for the production of iron and steel and unless it is upgraded to reduce its gangue content and increase its Fe content. The process adopted to upgrade the Fe content of iron ore is known as iron ore beneficiation (Satyendra, 2014a). The principal impurities being silica and moisture (Michaud, 2017).

Iron ores from different sources have unique mineralogical characteristics and therefore require the specific beneficiation and metallurgical treatment to get the best product out of it. The choice of the beneficiation treatment depends on the characteristics of the gangue present and how it is related to the ore structure. For effective beneficiation treatment to be achieved, effective crushing, grinding, and screening of the ore is necessary for which suitable crushing, grinding, and screening technologies must be used. Several methods/techniques such as washing, jigging, magnetic separation, gravity separation, and flotation, etc. are used to enhance the Fe content of the Iron ore and to reduce its gangue content. These techniques are used in various combinations for the beneficiation of iron ores (Satyendra, 2014a).

2.5.2 Agglomeration

With the increase in mechanized mining activity and the soft and friable nature of the ores, the generation of fines and ultra-fines has been steadily increasing. Also, the steps involved in the beneficiation process, handling, and transportation operation generate fines and ultra-fines. These fines and ultra-fines can be efficiently used for the production of iron and steel, if used in the form of pellets or sinters, either directly or after beneficiation (Patra and Rayasam, 2018). The formation of pellets and sinters is part of the agglomeration process.

Five iron ore agglomeration technologies can be defined. These are briquetting, nodulization, extrusion, pelletization and sintering. Sintering and pelletization are the most important agglomeration technologies (Fernández-González, et al., 2018). Pelletisation technique will be employed in this work.

Pelletisation is the unit operation of agglomerating iron bearing mineral fines (generally below 150 µm with 65-80% passing 40µm) by tumbling in horizontal rotating drums or inclined discs (Satyananda *et al.*, 2017). Others have shown that iron ore pellets from different pelletizing plants generated varying quantities of fine particles (< 600 µm) using a set of mechanically agitated screens (Copeland and Kawatra, 2005). Pellets are balls formed by rolling moist concentrates and fines iron ores of different mineralogical and chemical composition, with the addition of additives and binder, in a horizontal drum or an inclined disc. Pellets are obtained by adding an appropriate amount of water to the iron ore concentrate; this is a fundamental factor in the formation and growth of pellets, which creates a surface tension that holds the mineral grains cohesive, thus allowing their handling. Pellets produced to be used in ironmaking processes must have characteristics that meet the list of quality specifications regarding physical, chemical, and metallurgical properties. (Moraes, et al., 2018).

2.5.3 Reduction

Iron ore in its natural form can be used directly as a raw material for processing iron or low grade ore can be upgraded through beneficiation before it's charged into the

blast furnace (BF) or Direct Reduction (DR) furnaces (Muwanguzi *et al.*, 2012a). The BF is charged with metallurgical coke and iron-bearing materials separately, which leads to a layered structure. The iron-bearing materials consist of iron ore pellets, lump ore, and sinter. When the charge material descends, it is reduced by CO and H_2. In the ideal situation, iron-bearing materials reduce fast and remain in the solid form in as high temperatures as possible. The reduction of iron oxides occurs step wise from hematite to magnetite, magnetite to wüstite, and wüstite to metallic iron. Reduction occurs with CO and H_2 (Heikkilä *et al.*, 2020).

2.6 Iron Reduction in Iron Production

There are two possible ways of reduction of iron ore by solid carbon. These are direct reduction (where the iron in the ore reacts with solid carbon to produce iron) and indirect reduction (where the iron in the ore reacts with carbon monoxide) (Dutta and Chokshi, 2020). Carbon monoxide (CO) and hydrogen (H_2) are the most common reducing agents used in commercial processes (Sun, 1997).

2.6.1 Gasification of Carbon

Gasification of solid-state carbon takes place to produces CO

$$C_{(s)}+O_{2(g)}\rightarrow CO_{2(g)} \quad (1)$$

$$C_{(s)}+CO_{2(g)}\rightarrow 2CO_{(g)} \quad (2)$$

Any moisture present in the blast will also react with carbon

$$C_{(s)}+H_2O_{(g)}\rightarrow 2CO_{(g)}+H_{2(g)} \quad (3)$$

(Dutta and Chokshi, 2020)

2.6.2 Reduction of Iron Oxides by CO and H_2

Direct Reaction

$$Fe_2O_3 + 3C_{(s)} \rightarrow 2Fe + 3CO_{(s)} \quad (4)$$

$$Fe_3O_4+4C_{(s)}\rightarrow 3Fe+4CO_{(g)} \quad (5)$$

(Dutta and Chokshi, 2020)

Indirect Reaction

The reduction of Fe_2O_3 takes place in stages (above 570 °C),

$Fe_2O_3 \rightarrow Fe_3O_4 \rightarrow FeO \rightarrow Fe$:

From hematite to magnetite (around 500 °C)

$$3Fe_2O_3 + CO_{(g)} \rightarrow 2Fe_3O_4 + CO_{2(g)} \quad (6)$$

$$3Fe_2O_3 + H_{2(g)} \rightarrow 2Fe_3O_4 + H_2O_{(g)} \quad (7)$$

From magnetite to wüstite (between 600 and 900 °C)

$$Fe_3O_4 + CO_{(g)} \rightarrow 3FeO + CO_{2(g)} \quad (8)$$

$$Fe_3O_4 + H_{2(g)} \rightarrow 3FeO + H_2O_{(g)} \quad (9)$$

From wüstite to metallic iron (between 900 and –1100 °C)

$$FeO + CO_{(g)} \rightarrow Fe + CO_{2(g)} \quad (10)$$

$$FeO + H_{2(g)} \rightarrow Fe + H_2O_{(g)} \quad (11)$$

The main reaction is given below as

$$Fe_2O_3 + 3CO \rightarrow 2Fe + 3CO_2 \quad (12)$$

(Dutta and Chokshi, 2020; Heikkilä *et al.*, 2020).

2.6.3 Carburisation

Carburising is the addition of carbon to thesurface of low-carbon steels at temperatures (generally between 850 and 980°C) at which austenite, with its high solubility for carbon, is the stable crystal structure (Schneider, et al., 2013).Carburisation of the pure iron is required for lowering its melting temperature and obtaining a melt and slag separation at molten state (Anameric, et al., 2006). Some carburising equation are given in equations 13 and 14.

$$Fe_{(s)} + CO_{(g)} \rightarrow 2Fe_3C + CO_{2(g)} \quad (13)$$

$Fe_{(s)}+C_{(s)}\rightarrow 2Fe_3C$ (14)

(Dutta and Sah, 2016).

2.7 Technology for Iron Making

The blast furnace and the Direct Reduction are the methods by which iron is produced. The product of the blast furnace is pig iron whiles sponge iron is referred to iron produced from DR method (Muwanguzi *et al.*, 2012a).

2.7.1 Blast Furnace

The blast furnace is an efficient high-temperature reactor in which hot reducing gases formed from the combustion of coke and supplementary fuels in the raceway zone travel counter-current to the burden materials including iron ore, coke and fluxes charged in from the top (Gupta *et al.*, 2008). The principal objective of the blast furnace (BF) is to produce hot metal at a higher rate. The only critical operating parameter is the temperature of the hot metal and slag which must be greater than 1425 °C for these products to be tapped from the furnace in the molten state (Dutta and Chokshi, 2020).

The iron blast furnace is a tall, vertical shaft furnace which uses carbon, mainly in the form of coke to reduce iron ores. The product, a hot metal (which is impure iron), is suitable as feed material for steelmaking to refine it (Dutta and Chokshi, 2020). A schematic diagram is illustrated in Figure 2.3.

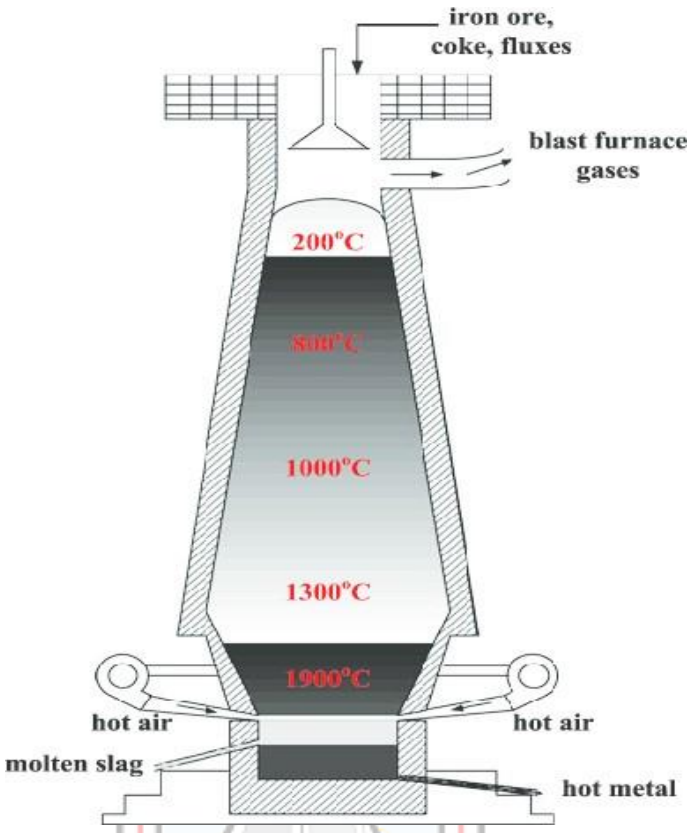

Figure 2.3 Schematic diagram of Blast Furnace

The principal raw materials used in the blast furnace operation consist of Metallurgical coke, ferrous bearing feeds and fluxes charged via the furnace top, Cold hydrocarbon fuels and hot oxygen-enriched air blast injected through the tuyeres near the furnace bottom. The blast furnace is a continuously operating shaft furnace based on the counter current flow principle (Bahgat *et al.*, 2012).

Metallurgical coke supplies most of the reducing gas and heat for ore reduction and smelting operation. The hot blast burns the descent coke in front of the tuyeres at 1525 °C to provide heat for reduction reactions and heating and melting of the charge materials and products, (hot metal and slag) (Dutta and Chokshi, 2020). The charged materials descend under the influence of gravity while the hot gas ascends through the furnace result in some vital functions. Therefore, the blast furnace can be considered as a counter current heat and mass exchanger as heat is transferred from the gas to burden and oxygen from burden to reducing gas. The counter current

nature of the reactions makes the overall process extremely efficient (Bahgat *et al.*, 2012).

2.7.2 Direct Reduced Iron (DRI)

DRI or sponge iron refers to porous iron produced by the DR process. The DR process is a solid-state reaction process (i.e., solid–solid or solid–gas reaction) in which removable oxygen is removed from the iron oxide, using coal or reformed natural gas as reductants, below the melting and fusion point of the lump ore or agglomerates of fine ore (Dutta and Sah, 2016). The external shape of the ore remains unchanged. Due to removal of oxygen, there is about 27–30% reduction in weight, a honeycombed microstructure remains which have suggested the name sponge iron (means solid porous iron, lumps/pellets, with many voids filled with air. Based on the types of reductant used, the sponge iron processes can be broadly classified into two groups: 1. Using solid reductant, i.e. coal-based direct reduction (DR) process, and 2. Using gaseous reductant, i.e. gas-based direct reduction (DR) process (Dutta and Chokshi, 2020).

2.7.3 Utilisation of Microwave in Laboratory Ironmaking

Microwaves are defined as a part of electromagnetic waves which have frequency range between 300 MHz and 300 GHz corresponding to wavelength from 1mm to 1m (Okeke, et al., 2005). For all practical purposes only 915 MHz and 2450 MHz are used for industrial ovens since components and power sources are readily available at these frequencies. All present day home microwave ovens in use are at 2450 MHz (Krieger and Tredinnick, 2002). Microwave energy is a non-ionizing electromagnetic energy characterized by mutually perpendicular electric and magnetic fields. The massive use of microwaves in thermal processing lays in the way the materials are heated. In contrast to conventional heating, microwave energy is delivered directly to the material through molecular interaction with the electromagnetic field. This difference in the way energy is delivered can result in many potential advantages to using microwaves for the processing of materials, such as uniform heating of complex shaped materials, effective heating of materials with low conductivity, selective

heating of distinct phases that couple with microwaves (Panias and Krestou, 2004). There are essentially two mechanisms for the absorption of microwave power by materials. One is that of dipole rotation which would apply to polar materials. The second mechanism of microwave heating is that of ionic conduction (Krieger and Tredinnick, 2002).

As a general rule, there are three types of interaction between materials and microwave energy. These are transmission through the material, reflection by the material and absorption by the material. Fortunately, many minerals and ores can absorb microwave energy to a greater or lesser extent and be heated in the process (Standish and Huang, 1991). The maximum temperature of some oxide and sulfide compounds when heated with microwave is given in Table 2.3.

Table 2.3 Microwave heating of some oxide and sulfide compounds

Compound	Heating time (min)	Max. Temp. (°C)
Al_2O_3	24	1900
C	0.2	1000
CaO	40	200
Co_2O_3	3	900
CuO	4	800
CuS	5	600
Fe_2O_3	6	1000
Fe_3O_4	0.5	500
FeS	6	800
MgO	40	1300
MoO_3	0.46	750
MoS_2	0.1	900
Ni_2O_3	3	1300
PbO	13	900
UO_2	0.1	1100

(Source Koleini and Barani, 2012)

The applications of microwave energy for the reductions of metal oxides with carbon for ironmaking was experimented. In these experiments, identical samples of hematite ore fines, coke dust and lime powder was used. some of which reduced conventionally at 1000 °C and others in a microwave oven at 1.3 kW with a frequency of 2.45 GHz. The results obtained showed that microwave heating resulted in a 16% increase of weight loss over conventional heating, while no "cold centers" occurred in the treated ore (Standish and Huang, 1991). Microwave energy is advantageous in the reduction of pre-oxidised Ilmenite concentrates (Panias and Krestou, 2004). Microwave technology was applied to the Production of Iron Nuggets from the Sheini Iron Ore (Dankwah *et al.*, 2018).

2.8 Reducing Agent

The reduction process in ironmaking is achieved with aid of reducing agent. Carbon-bearing materials are used as chemical reducing agents and as source of energy in the iron-making processes. Coke is the major reductant in iron-making. There are alternative carbon-bearing materials that are commercially available or still under development will be given. The alternative carbon-bearing materials should maintain the following properties which are Low contents of sulfur, phosphorus, and alkali, Moisture content, Volatile content, Controlled hardness or grindability , High solid or fixed carbon content, low ash, and high heating value. Among the alternative carbon bearing material are active (nut) coke, in-plant fines, bio-based carbon-bearing materials, waste plastic materials, carbon composite agglomerates, and End-of Life rubber tyres (Hesham, 2018).

2.8.1 Metallurgical Coke

When coking coals in coherent beds are heated in absence of air, they release volatiles and form strong and porous mass that are known as coke. Coke, produced out of coal, contains 21.12% ash, 78% fixed carbon, 0.88% volatile matter, 0.18% P, 0.57% S and 1.4% moisture. Coke with these specifications may be considered as good coke (Dutta and Chokshi, 2020). Coke is usually produced in by-product coke ovens by destructive distillation of coal. High-quality blast furnace coke must have low and

consistent moisture content, low content of impurities, high strength, relatively low reactivity and a uniform size range. These properties are mainly governed by a proper mix of suitable coals and the optimization of the coking conditions which are coal size, bulk density and coke oven heating rate (Lundgren, 2010). Table 2.4 lists the properties of a metallurgical coke.

Table 2.4 Properties of metallurgical coke

Component	Carbon	Hydrogen	Sulphur	Nitrogen	Calorific Value mJ/kg
Content	77.7	1.11	0.28	1.21	28-31

2.8.2 End of Life Vehicle Tyres

Tyres differ in size and design according to their use and producer. However, the composition is very almost the same (Ramos, et al., 2011). Passenger car, lorry and off-the-road ("OTR") tyres are products of complex engineering. They are made up of numerous different rubber compounds, many different types of carbon black, fillers like clay and silica, and chemicals and minerals added to allow or accelerate vulcanisation. The tyres also have several types of fabric for reinforcement and several kinds and sizes of steel. Some of the steel is twisted or braided into strong cables (Evans and Evans, 2006). End-of-life tyres (ELT's) refers to tyres that have surpassed their useful lifespan in terms of roadworthiness, that is, tyres that had burst or have been utterly damaged beyond a safety limit for usage in vehicles for transport due to degeneration of certain properties like eccentricity, flat and balanced surface, grip surface among others (Ishola *et al.*, 2018). Different tyres have different composition as shown in Table 2.5.

Table 2.5 Composition of Tyres (Evans and Evans, 2006).

INGREDIENT	PASSANGER CAR TYRE (%)	LORRY TYRE (%)	OTR TYRE (%)
Rubber	47	45	47
Cardon Black	21.5	22	22
Metal	16.5	25	12
Textile	5.5	-	10
Zinc Oxide	1	2	2
Sulphur	1	1	1
Additives	7.5	5	6
Carbon-Based Materials, Total	74	67	76

The most common rubbers used in the manufacture of tyres are cis-polybutadiene rubber (CBR), isobutylene-isoprene copolymer rubber (i.e., butyl rubber (BR)) and styrene-butadiene copolymer rubber (Ramirez-Canon, et al., 2018).

Butyl rubber (IIR) is the copolymer of isobutylene and low levels of isoprene, which is commercially produced by cationic polymerization (Bonilla-Cruz *et al.*, 2017). This cationic copolymerization of isobutylene and isoprene occurs in chloromethane solution in the presence of $AlCl_3$ as catalyst and water or HCl as cocatalyst at temperature under – 90 °C (Anon, 2007). Figure 2.4 shows the chemical structures of butyl rubber.

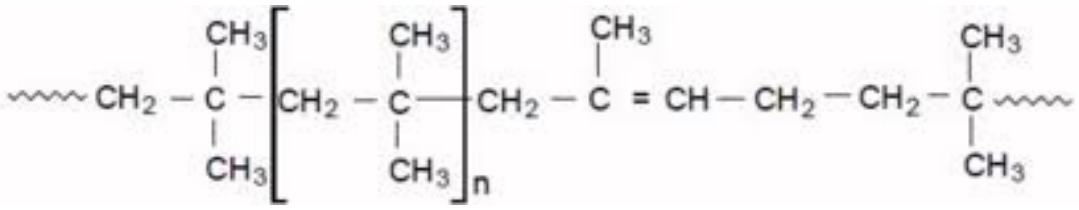

Figure 2.4 Butyl Rubber Structure

Styrene-butadiene rubbers (SBR) are copolymers of styrene and butadiene. They are of the most commonly used rubbers. Their properties are influenced not only by micro- and macrostructure of polymer chains but also by styrene content. Butadiene structural units can be arrangement as cis-1.4, trans-1.4 or 1.2 (vinyl) units. Mutual arrangement of styrene and butadiene units can have random, partially-block or block character. SBR do not crystallize even under stress, hence, influence of mutual arrangement of „cis" and „trans" units on their properties is lower than it is in the case of BR (Anon, 2007). The most important application of SBR is in car tires and tire products, but there is also widespread use of the rubber in mechanical and industrial goods. SBR latexes, which are emulsions of styrene–butadiene copolymers (containing about 23–25% styrene), are used for the manufacture of foam rubber backing for carpets and for adhesive and molded foam applications (Chanda, 2018). Figure 2.5 shows chemical structure of styrene-butadiene.

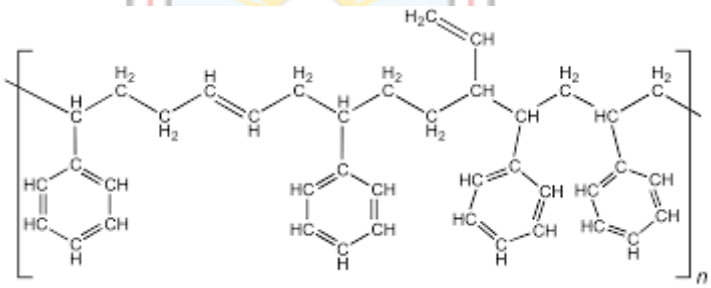

Figure 2.5 Styrene Butadiene Structure

Polybutadiene is made by solution polymerization of butadiene using Ziegler–Natta catalysts. Slight changes in catalyst composition produce drastic changes in the stereoregularity of the polymer. For example, polymers containing 97–98% of trans-1,4 structure can be produced by using Et_3Al/VCl_3 catalyst, those with 93–94% cis-1,4 structure by using $Et_2AlCl/CoCl_2$, and those with 90% 1,2-polybutadiene by using $Et_3Al/Ti(OBu)_4$. The stereochemical composition of polybutadiene is important if the product is to be used as a base polymer for further grafting. For example, a polybutadiene with 60% trans-1,4, 20% cis-1,4, and 20% 1,2 configuration is used in the manufacture of ABS resin (Chanda, 2018).

Polybutadiene rubbers generally have a higher resilience than natural rubbers at room temperature, which is important in rubber applications. On the other hand, these rubbers have poor tear resistance, poor tack, and poor tensile strength. For this reason polybutadiene rubbers are usually used in conjunction with other materials for optimum combination of properties. For example, they are blended with natural rubber in the manufacture of truck tires and with styrene–butadiene rubber (SBR) in the manufacture of automobile tires (Chanda, 2018). The structure of cis-polybutadiene is illustrated in Figure 2.6.

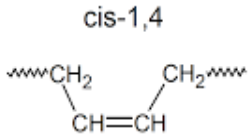

Figure 2.6 cis-polybutadiene structure

Almost all rubbers require vulcanization which is a process that rubber is transformed from elastic into plastic material (Fragassa and Ippoliti, 2016). Vulcanization imparts strength, stiffness, and modulus, as well as resistance to fatigue and abrasion (Lim and Sirisomboon, 2017). Sulfur is one of the most common vulcanization agents used in the rubber industry which used for natural and many synthetic types of rubber (Shahrampour, 2018).

Polymers are made of hydrocarbon which makes them rich in carbon and hydrogen atoms (Kondrin, et. al. 2016). Table 2.6 compares the properties of metallurgical coke to rubber.

Table 2.6 Comparison of Metallurgical coke, and Rubber (Sahajwalla *et al.*, 2011)

COMPONENTS	METALLURGICAL COKE (MC)	RUBBER
Carbon%	77.7	85.48
Hydrogen%	1.11	6.9
Sulphur%	0.28	1.68
Nitrogen%	1.21	0.25
Calorific Value MJ/kg	28-31	40.1

2.8.3 Utilisation of end-of-Life Tyres in Ironmaking

From table 2.2 and 2.3 it can be concluded that ELTs have the potential of replacing coke or to be used in combination in iron making. This have led series to researches in the ironmaking industry. Billions of ELTs currently held in various stockpiles across the globe can be diverted for use as source of carbon for slag foaming in EAF steelmaking. Studies conducted by previous researches have shown that blends of rubber with metallurgical coke could be used to partially replace some of the conventional metallurgical coke used in EAF steelmaking for its injecting carbon requirements and improvements in the slag foaming behaviour and furnace efficiency (Dankwah *et al.*, 2012; Zaharia *et al.*, 2012; Dankwah and Koshy, 2013; Dankwah, 2018). In a study by Sahajwalla et al., 2011, it was demonstrated that recycled plastics and tyres can be used as alternative carbon sources for slag foaming in EAF steelmaking. Abotar, 2019, in his research work concluded that ELTs were excellent potential source of carbonaceous material for iron oxide reduction in the Pudo iron ore.

In this research, the response of Opon Mansi iron ore to reduction by ELTs was conducted.

CHAPTER 3
MATERIALS AND METH0DS

3.1 Materials

3.1.1 Raw Materials Used

The raw materials used in doing this work were the Opon Mansi iron ore from Opon Valley in the Western Region of Ghana, Non-Magnetic iron ore from the Pudo Mountains in the Upper West Region of Ghana, End-of-life vehicle tyre (ELT) obtained from a vulcaniser shop from Tarkwa and flour, which was obtained from the Tarkwa local market served as a binder.

3.1.2 Apparatus Used

The experimental section of the work was conducted at the University of Mines and Technology Minerals Engineering laboratory while the elemental analysis was conducted at the Mark Wainwright Chemical Laboratory, University of New South Wales, Sydney, Australia. The laboratory-based equipment used for this work included the Jaw, Cone and Roll crushers, ball mill, Electronic balance, Domestic Microwave Oven (BINATONE, 1050 W input, 2450 MHz) and a low intensity magnet. According Copeland and Kawatra, 2005, varying fine particles sizes <600 µm are generated in iron ore pelletizing plants, hence 250 µm sieve was used in this work.

3.2 Methods

This research was done using the following methods:

a. Sampling of Iron ore
b. Sample Preparation
c. XRD, XRF, and SEM-EDS Analysis
d. Pelletisation
e. Reduction Studies

3.2.1 Sampling of Iron Ore

Samples taken from three different sites in Opon Mansi which were labelled A, B and C were considered for this project. Each sample weighing about 15 kg was randomly taken by grab sampling technique. About 2 kg each of the different samples from Opon Mansi and about 50 g of the Pudo non-magnetic ore were used for the work.

3.2.2 Sample Preparation

The Opon Mansi samples ranged within particle size distribution of about 5-15 mm. Since most of the ore particles were relatively fine (about 5 mm), the coarser ones were jaw and cone crushed to obtain a size of about 5 mm as well. Tertiary crushing was also done using a Roll crusher to obtain sizes of about 1.6 mm-2.4 mm. The samples were further milled using the Ball mill for about 30 minutes after which it was screened with a 250 µm sieve to obtain 100% passing 250 µm shown in Figure 3.1

Figure 3.1 Pulverised Samples of Opon Mansi Iron Ore (-250 *µm*)

The Pudo non-magnetic iron ore was already prepared; thus was screened to obtain -250 µm of the material as shown in Figure 3.2

Figure 3.2 Sample of Pulverised Pudo Non Magnet Iron Ore (-250 µm)

3.2.3 Reducing Agent Preparation

End-of-life vehicle tyre was used as the reducing agent for this work since recycled plastics and tyres can be used as an alternative carbon source (Sahajwalla *et al.*, 2011). Charring was done to eliminate any volatile components to concentrate the carbon which was going to perform the reduction.

Charring was done using an enclosed container with a single perforation at the top, for about 30 minutes and further taken through grinding and screening. The material was then screened through the 250 µm sieve to obtain -250 µm shown in Figure 3.3

Figure 3.3 Sample of Charred End-of-Life Tyre

3.2.4 Pelletisation and Reduction Studies

The sequence of steps carried out in this work included the calculation on the amount of each component involved in the pellet formation, drying under room temperature, microwave heating of the dry pellets and weighing of masses. These steps are described below.

Formation of Pellet

The pellet had a total mass of 30 g. This was made up of 70% Iron ore, 28% Reducing agents and 2% Binder. Based on these percentages, 21 g of the Iron ore, 8.4 g of the reducing agent, and 0.6 g of flour was used in all pellet formation in the experiment.

The pellets used for this work were all formed in a plastic bowl. The formation of pellets was done in two separate sections.

The iron ore used in the formation of the pellets for the first section was solely the Opon Mansi ore. 60 pellets were formed in all i.e. (20 pellets each for the 3 sampling areas A, B and C respectively). The different components of the pellets (ore, ELT and flour) were mixed thoroughly in the plastic bowl according to their various proportions and sprinkled with water in a water bottle. The wet materials by the aid of flour as the binding agent were then moulded into spherical balls in each case to get the pellets as shown in Figure. 3.4.

Figure 3.4 Formed pellets with the Opon Mansi Iron Ore

The iron ore used in the pellet formation for the second section comprised the Pudo non-magnetic and Oppong Mansi iron ores. These pellets were formed in different proportions as shown in the Table 3.1.

Table 3.1 Blend Ratio of the Magnetic, Non-Magnetic Iron Ore and ELT(S) Used in the Reducibility Studies

SAMPLE ID	**IRON ORE 70%**		**IRON ORE IN GRAMS**		**CARBONACEOUS MATERIAL 30%**		**CARBONACEOUS MATERIAL (G)**	
CODE	MAGNETIC	NON MAGNETIC	MAGNETIC	NON MAGNETIC	ELTS	BINDER	ELTS	BINDER
A	100%	0%	21.00	0.00	28%	2%	8.40	0.60
B	90%	10%	18.90	2.10	28%	2%	8.40	0.60
C	85%	15%	17.85	3.15	28%	2%	8.40	0.60
D	80%	20%	16.80	4.20	28%	2%	8.40	0.60
E	75%	25%	15.75	5.25	28%	2%	8.40	0.60
F	70%	30%	14.70	6.30	28%	2%	8.40	0.60
G	60%	40%	12.60	8.40	28%	2%	8.40	0.60
H	50%	50%	10.50	10.50	28%	2%	8.40	0.60

XRF analysis, indicated that the distribution of iron in the samples A, B and C were 21%, 21% and 41% respectively. Since A and B were below the economically recoverable grade the reducibility test was conducted on only sample C.

Drying of Formed Pellets

The formed pellets were dried at room temperature for 7 days. Allowing the pellets to dry under room temperature helps to maintain the original chemical composition of the pellets. The drying allowed the moisture in the pellets to be removed completely and further gave the pellets the required strength for the firing process.

3.2.5 Reduction of Iron Ore-ELT Composite Pellets

The dry pellets were then subjected to a 1050 W input, 2450 MHz, BINATONE microwave oven. Prior to this, a spot was located in the microwave where there was maximum heating. For the first section, the firing was done at varying times (i.e. 20, 30, 40, 50 and 60 mins). At a particular firing time, say 20 mins, 3 pellets were fired. Each pellet was placed in a fireclay crucible and subjected to microwave heating, after which it was removed from the microwave and poured out of the crucible for cooling. Same was applied for the other set of samples. The pellets from the second section were all subjected to microwave heating for 60 minutes since it was found to be the best reduction time in section one. Before the pellet was placed in the crucible, a bed of reducing agents (Charred Palm Kernel Shells) was formed in the crucible. This was done to prevent likely reaction of the ore and crucible to form a slag. Figure 3.5 shows a sample of the reduced iron ore.

Figure 3.5 Samples of Reduced Iron Ore

3.2.6 Weighing of Masses

The masses of each pellet before and after the firing process were obtained using the electronic balance. The masses of the magnetic portions, the associated slags and the residual value of the reduction process were obtained to help ascertain the extent of the reduction process in the various pellets.

3.2.7 Gas Reduction Studies in a Horizontal Resistance Tube Furnace

Spherical pellets were formed from pulverised iron ore and charred ELT (~ 30 wt %) with about 2 wt % flour as binder and without flux addition (Figure 3.6).

The experimental apparatus consisted of a gas analyser connected to an electrically heated horizontal tube furnace (HTF) and a data logging computer (Figure 3.7). CO, and CO_2 were monitored continuously by an IR gas analyser (Advance Optima model ABB^® AO2020).

The iron ore-ELT composite pellet was placed in a LECO crucible prior to being fired in the HTF. The furnace was purged continuously with argon gas (99.995% purity) to ensure an inert atmosphere. The furnace was preheated to the desired temperature and the sample was inserted; gas measurement commenced immediately after insertion and continued for 2400 s. No appreciable change in gas composition was observed beyond 2400 s.

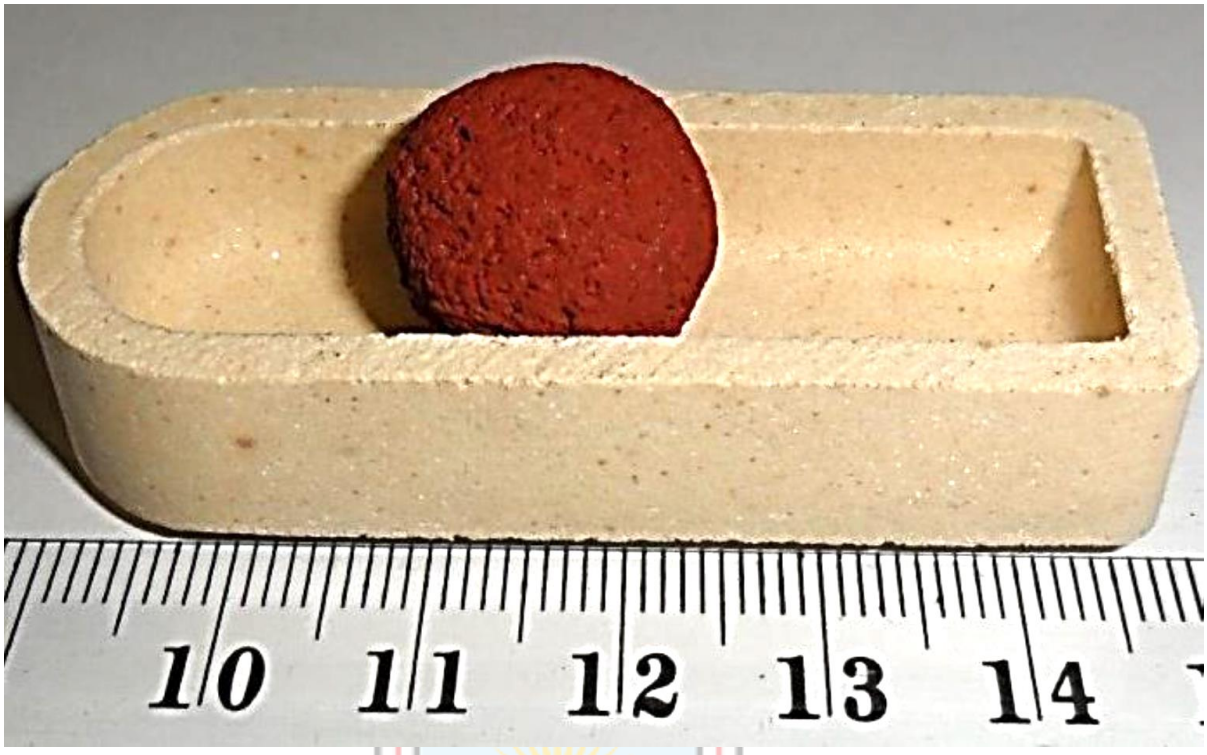

Figure 3.6 Iron ore-ELT Composite Pellet in a LECO™ Crucible

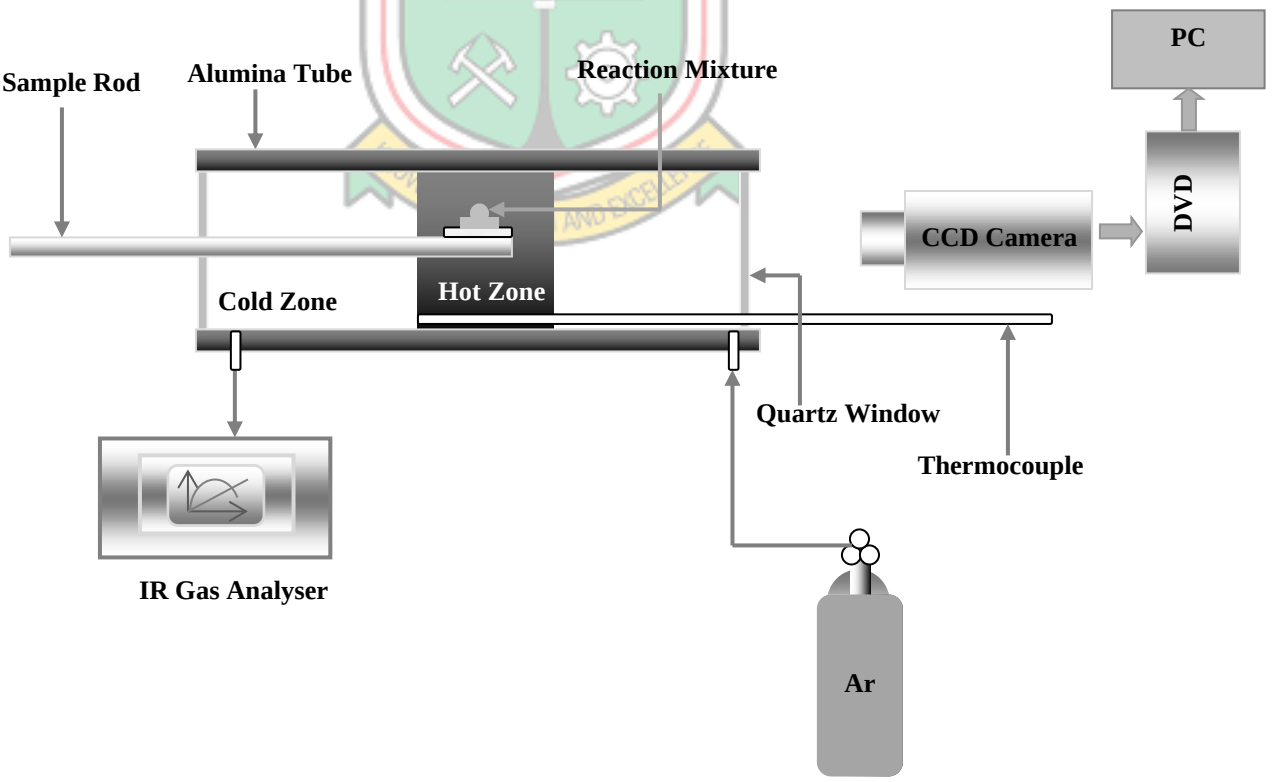

Figure 3.7 Schematic diagram of the horizontal tube furnace and IR gas analyser system

3.2.7 Extent of Reduction from Off-Gas Data

The off-gas data was generated continuously. Accordingly the overall rate of gas generation could be described by a continuous function R_o (mol s^{-1}), from which the extent of reduction can be estimated by integration (Dankwah *et al.,* 2011). In that case the extent of reduction (*f*) after time *t* can be calculated from equation (3.1):

$$f = \frac{1}{N_o}\int_0^t R_o.dt \qquad (3.1)$$ (Dankwah *et al.,* 2011)

where N_o is the total amount of reducible oxygen in converting the iron oxide from (Fe_2O_3) to Fe.

R_o can be estimated from the individual molar fluxes, J_i, (mol cm^{-2} s^{-1}) as shown in equation (3.2), assuming that the gases behave ideally (room temperature = 20 °C):

$$J_i = \frac{273}{293} \times F_{Ar} \times \frac{\%i}{22.4 \times \%Ar} \cdot \frac{1}{A} \qquad (3.2)$$ (Dankwah *et al.,* 2011)

From a mass balance for oxygen (based on complete transformation of (Fe_2O_3) to Fe), the flux of O is calculated from equation 3.3.

$$-J_O = J_{CO} + 2 \cdot J_{CO_2} + J_{H_2O} \qquad (3.3)$$ (Dankwah *et al.,* 2011)

The rate of removal of O from Fe_2O_3 is thus given by equations 3.4 and 3.5:

$$R_o = -\frac{d(n_O)_t}{dt} = -AJ_O \qquad (3.4)$$ (Dankwah *et al.,* 2011)

$$R_o = 0.0416 \times F_{Ar} \times \left(\frac{2 \times \%CO_2}{\%Ar} + \frac{\%CO}{\%Ar} + \frac{\%H_2O}{\%Ar} \right) \qquad (3.5)$$ (Dankwah *et al.,* 2011)

Where: J_i, n_o, F_{Ar} and *A* are the molar flux (mol of species i/cm^2.sec), amount of O (mol) at time t, Ar flow rate (F_{Ar} = 1.0 L/min) and reaction area (cm^2) respectively.

Equation 3.5 can usually be approximated by equation 3.6 at temperatures above 700 °C and C/O > 1.0, where $\%H_2O \sim 0$ (Dankwah *et al.,* (2011); Rezan *et al.,* 2012); Dankwah *et al.,* (2017).

$$R_o \approx 0.0416 \times F_{Ar} \times \left(\frac{2 \times \%CO_2}{\%Ar} + \frac{\%CO}{\%Ar} \right) \quad (3.6) \quad \text{(Dankwah } et\ al.,\ 2011)$$

Based on the amount of removable oxygen from the ore, the extent of reduction, *f* can be expressed by equations 3.7-3.9.

$$f = \frac{amount\ of\ oxygen\ removed}{total\ amount\ of\ removable\ oxygen} \quad (3.7) \quad \text{(Dankwah } et\ al.,\ 2017)$$

$$f = \frac{n_{CO} + 2n_{CO_2} + 2n_{H_2O}}{N_O} \quad (3.8) \quad \text{(Dankwah } et\ al.,\ 2011)$$

Again, under the conditions of the experiment, $nH_2O \sim 0$. Consequently, the extent of reduction can be approximated by equation 11.

$$f \approx \frac{n_{CO} + 2n_{CO_2}}{N_O} \quad (3.9) \quad \text{(Dankwah } et\ al.,\ 2017)$$

CHAPTER 4

RESULTS AND DISCUSSION

4.1 Nature of the Opon Mansi Ore

4.1.1 X-Ray Diffraction Analysis analysis of the Ore

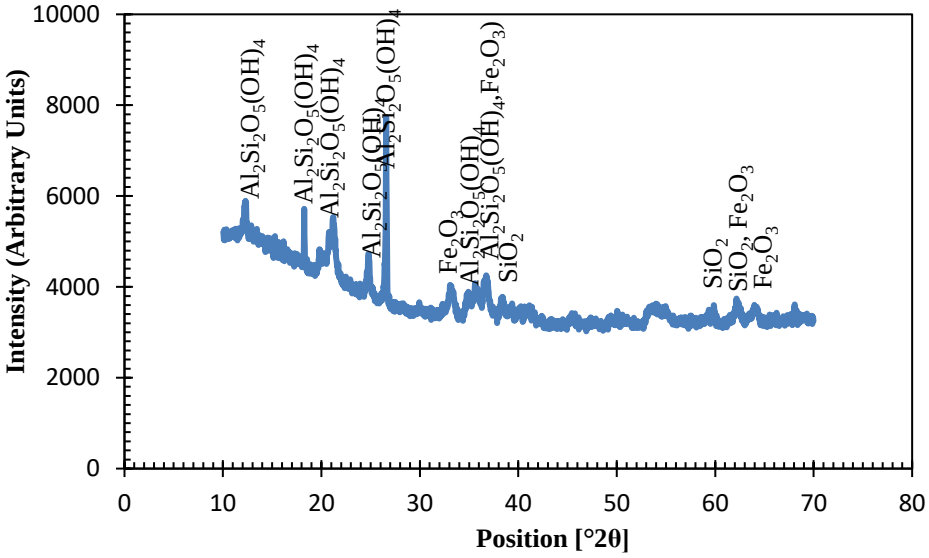

Figure 4.1 X-Ray Diffractogram of the Ore utilised for the Investigation

The minerals in the ore sample was characterised by XRD. In Figure 4.1 it was observed that highest intensity of peaks is of hematite, silica, and alumina. The diffracted patterns show that iron exists only as hematite, classifying the ore as a hematite ore. The major gangue minerals as shown in the diffractogram are SiO_2 and Al_2O_3.

4.1.2 SEM-EDS Analysis of the Ore

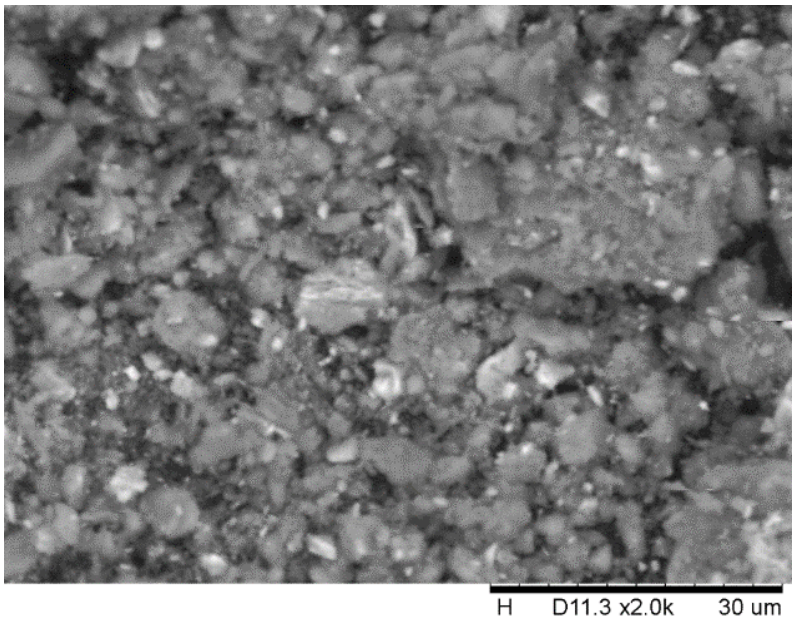

Figure 4.2 Scanning Electron Micrograph (×500) of the Ore utilised for the Investigation

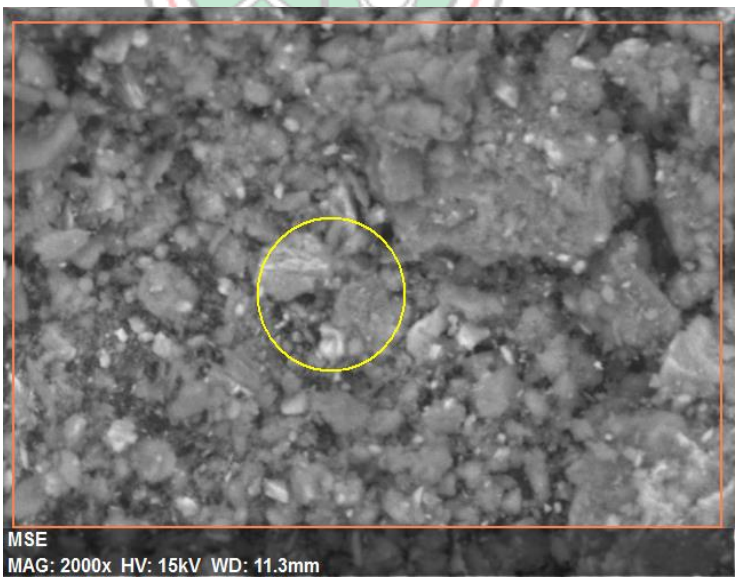

Figure 4.3 Scanning Electron Micrograph (×2.0k) of the Ore utilised for the Investigation

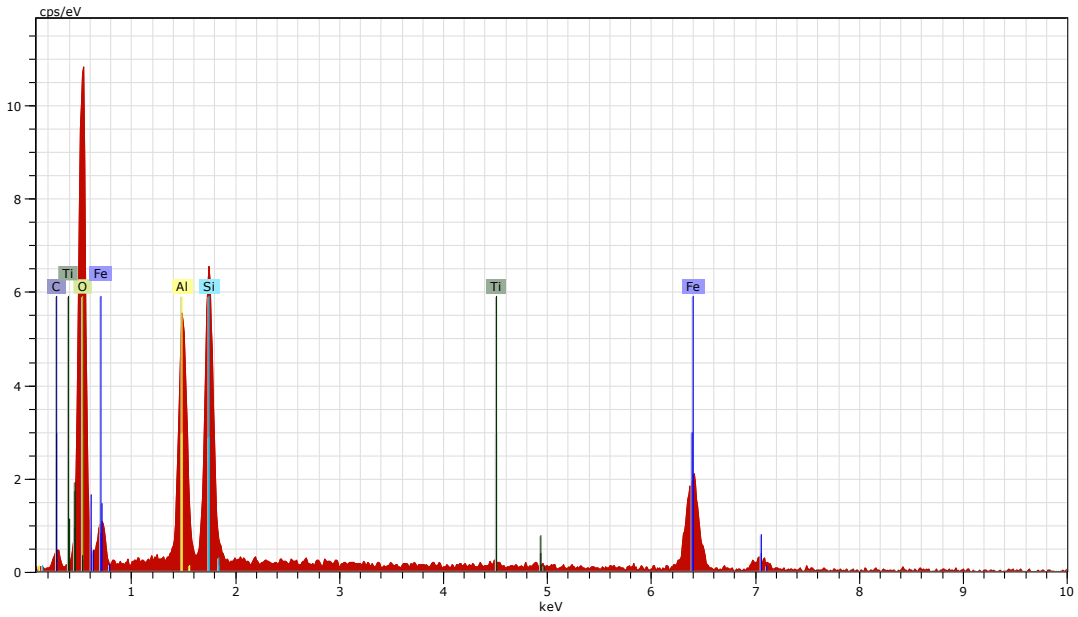

Figure 4.4 SEM/EDS Analysis of the Ore utilised for the Investigation

SEM investigations were conducted to identify the morphological conditions and homogeneity of the iron sample in Figures 4.2 and 4.3. The particles appeared to be irregularly shaped with clumps in them. Hence the morphological conditions are inhomogeneous. The peaks in the EDS spectra in Figure 4.4 above also shows that iron oxide (FeO), silicon oxide and aluminum oxide compounds are the major compound present in the sample. There were also trace of tin and carbon.

4.1.3 X-Ray Florescence (XRF) analysis of The Ore

Table 4.1 Chemical Composition by XRF of the Opon Mansi Ore

Component	Composition (%)	Component	Composition (%)
Al_2O_3	19.00	V_2O_5	0.08
SiO_2	24.97	Mn_3O_4	0.02
P_2O_5	0.12	Fe_2O_3	41.07
Cr_2O_3	0.01	NiO	0.01
TiO_2	1.26	LOI	13.37
SO_3	0.08	TOTAL	99.98

The chemical composition of raw iron ore is used to determine its quality and viability for commercial exploitation. The content of Fe, gangue (SiO_2 and Al_2O_3) and contaminations such as P and S are the most important elements and components of consideration in iron ores (Muwanguzi *et al.*, 2012b).

It was observed that the ore occurs as haematite ore with high gangue minerals content. The hematite content is 41.07% which has an iron content of 28.75%. This classifies the ore as a low-grade hematite ore. But for the ore to be economically recoverable the iron content must be greater than 25% (Palacios, 2011; Ofoegbu, 2019).

It was observed that the silica and natural alumina contents are 24.97% and 19% respectively. According to Kiptarus et al. (2015), generalized contents for SiO_2 and Al_2O_3 requirements in commercial iron ores are 6% and 3-4% respectively. However, the presence of 12–19% Al_2O_3 in the slag gives the desired fluidity for removal of sulphur from hot metal (Dutta and Chokshi, 2020). High alumina content will increase the viscosity of slag formed. The alumina to silica ratio that is higher than one poses serious operational problems during sintering and later smelting in the blast furnace (Rao *et al.*, 2009; Muwanguzi *et al.*, 2012b). But the alumina to silica ratio in this experiment was less than one.

It was observed that the SO_3 content was 0.08%. This means that the sulphur content is 0.03%. Phosphorus content in P_2O_5 observed to be 0.05%.

The titanium oxide content was observed as 1.26%. Iron ores which have TiO_2 content above 5% are not saleable. Since the observed TiO_2 content is lower than 5% it can be sold if all other factors are favourable.

4.2 Reduction of Opon Mansi Ore by ELT

4.2.1 Extent Reduction of 100% Hematite Opon Mansi Ore

The result of the extent of reduction of the ore by charred ELTs is plotted in a graph in Figure 4.5.

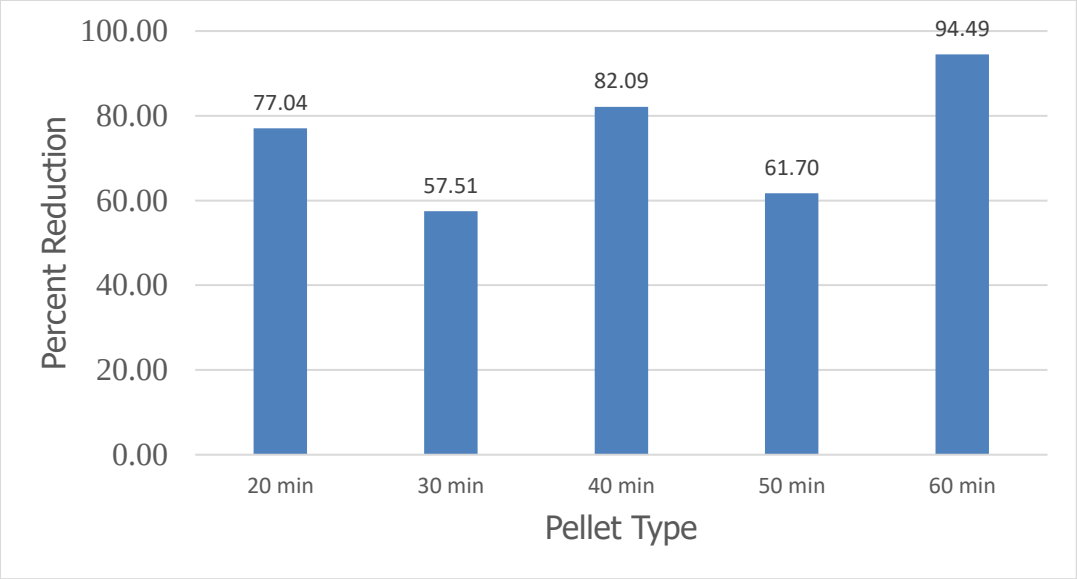

Figure 4.5 Graph of Percent Reduction Against Duration for reduction of composite sample C

From Figure 4.5 it can be observed that the extent of reduction of composite sample C ranged between 57% and 94%. The highest reduction occurring at 60 minutes of firing. But at 30 mins and 50 mins there was a dip in extent of reduction.

4.2.2 Extent of Reduction of Blended Opon Mansi Hematite Ore and Pudo Non-Magnetic Ore

The high contents of MgO and CaO in the Pudo non-magnetic ore makes a good fluxing agent. Hence to complement for the low MgO and CaO content in the Opon Mansi iron ore, the ore was blended with pulverised samples of the Pudo non-magnetic ore to assess the effectiveness of the latter as a possible fluxing agent. The extent of reduction was plotted as a function of the level of blending of the Opon Mansi ore with the Pudo non magnetic ore, as illustrated in Figure 4.6. From Figure 4.6, the blend of Opon Mansi and Pudo non-magnetic ores did not significantly improve on the extent of reduction, which ranged between 77% and 94%. The current results are in sharp contrast with the observation of Abotar *et al.*, (2020), that addition of the Pudo non-magnetic ore to the Pudo magnetic ore produced an excellent fluxing effect on the reduction of the latter by ELT.

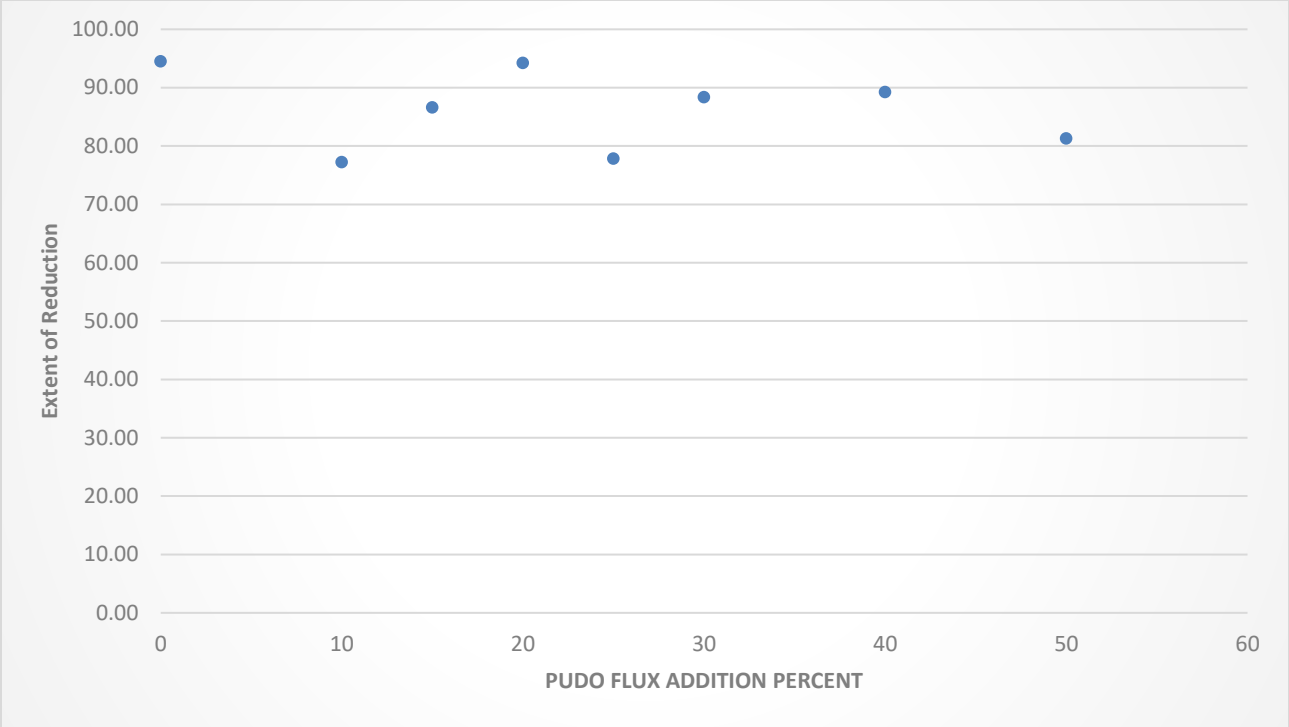

Figure 4.6 A graph of Extent of reduction against pellet blend (Pudo Flux) percent

4.2.3 Characterisation of Reduced Metal (Results of SEM/EDS Analysis)

The result of the SEM/EDS analysis on the reduced metal at 60 min. is given in Figures 4.7 to 4.11. The results of the elemental analysis on the reduced meteal is also represented in Tables 4.2 to 4.6.

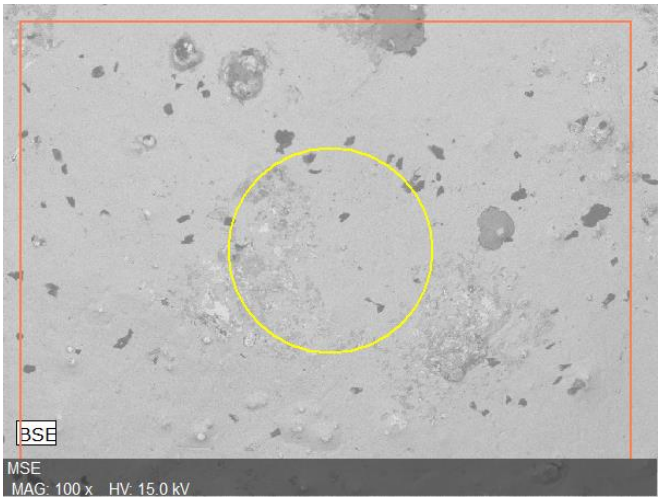

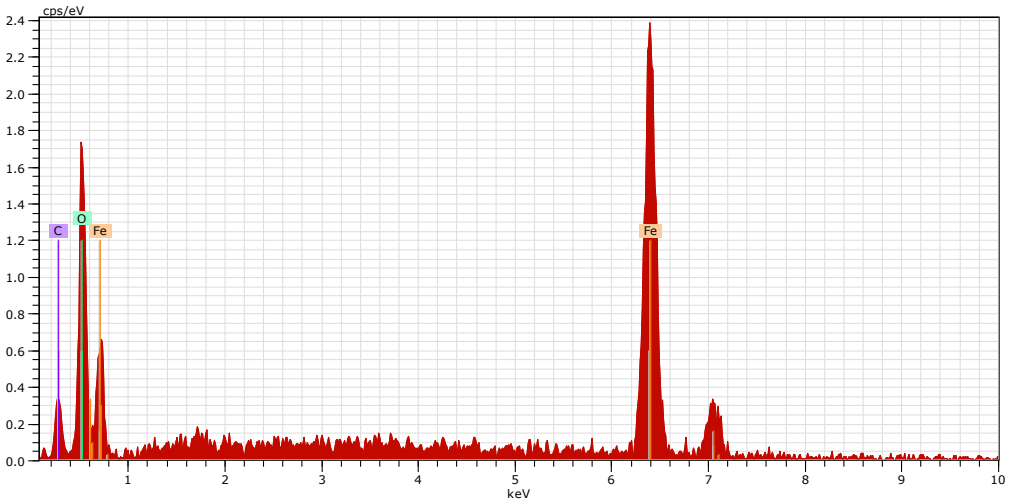

Figure 4.7 SEM/EDS Analysis of Reduced Iron Ore-ELT Composite Pellet (Region 1)

Table 4.2 Elemental Analysis of Region 1

Element	Mass %	Atom %
Fe	71.48	39.21
O	18.82	36.04
C	9.70	24.75
Sum	100.00	100.00

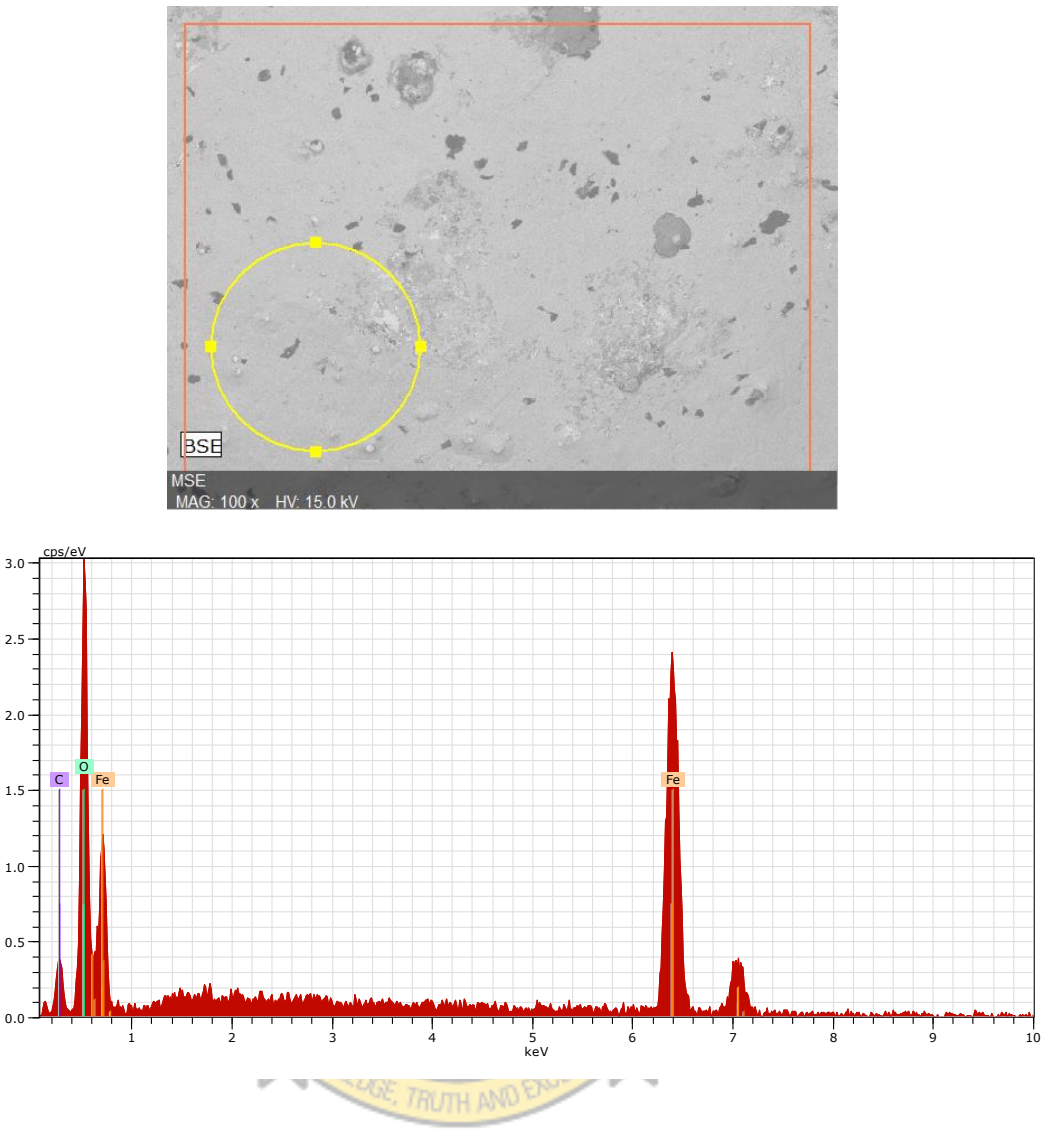

Figure 4.8 SEM/EDS Analysis of Reduced Iron Ore-ELT Composite Pellet (Region 2)

Table 4.3 Elemental Analysis of Region 2

Element	Mass %	Atom %
Fe	64.83	32.77
O	26.36	46.52
C	8.81	20.71
Sum	100.00	100.00

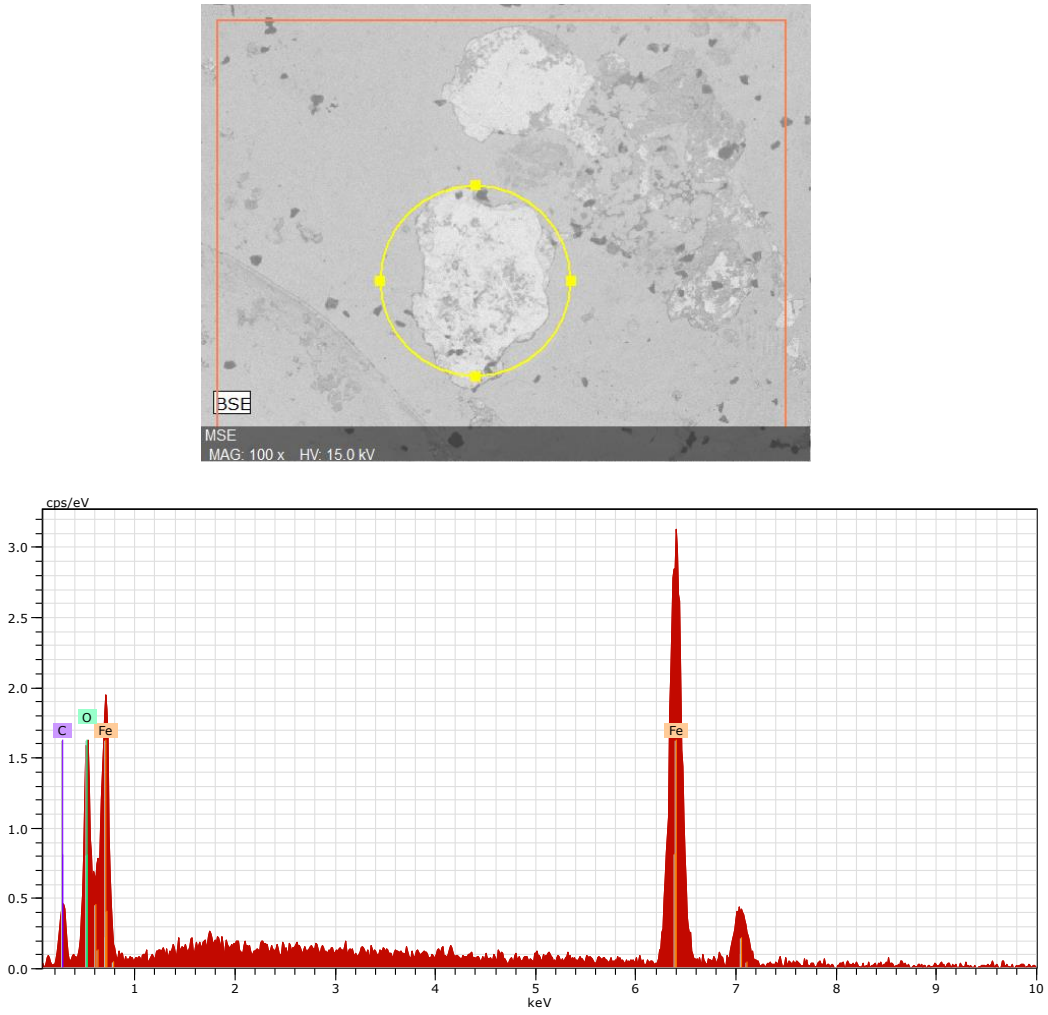

Figure 4.9 SEM/EDS Analysis of Reduced Iron Ore-ELT Composite Pellet (Region 3)

Table 4.4 Elemental Analysis of Region 3

Element	Mass %	Atom %
Fe	75.69	43.88
O	14.03	28.39
C	10.29	27.73
Sum	100.00	100.00

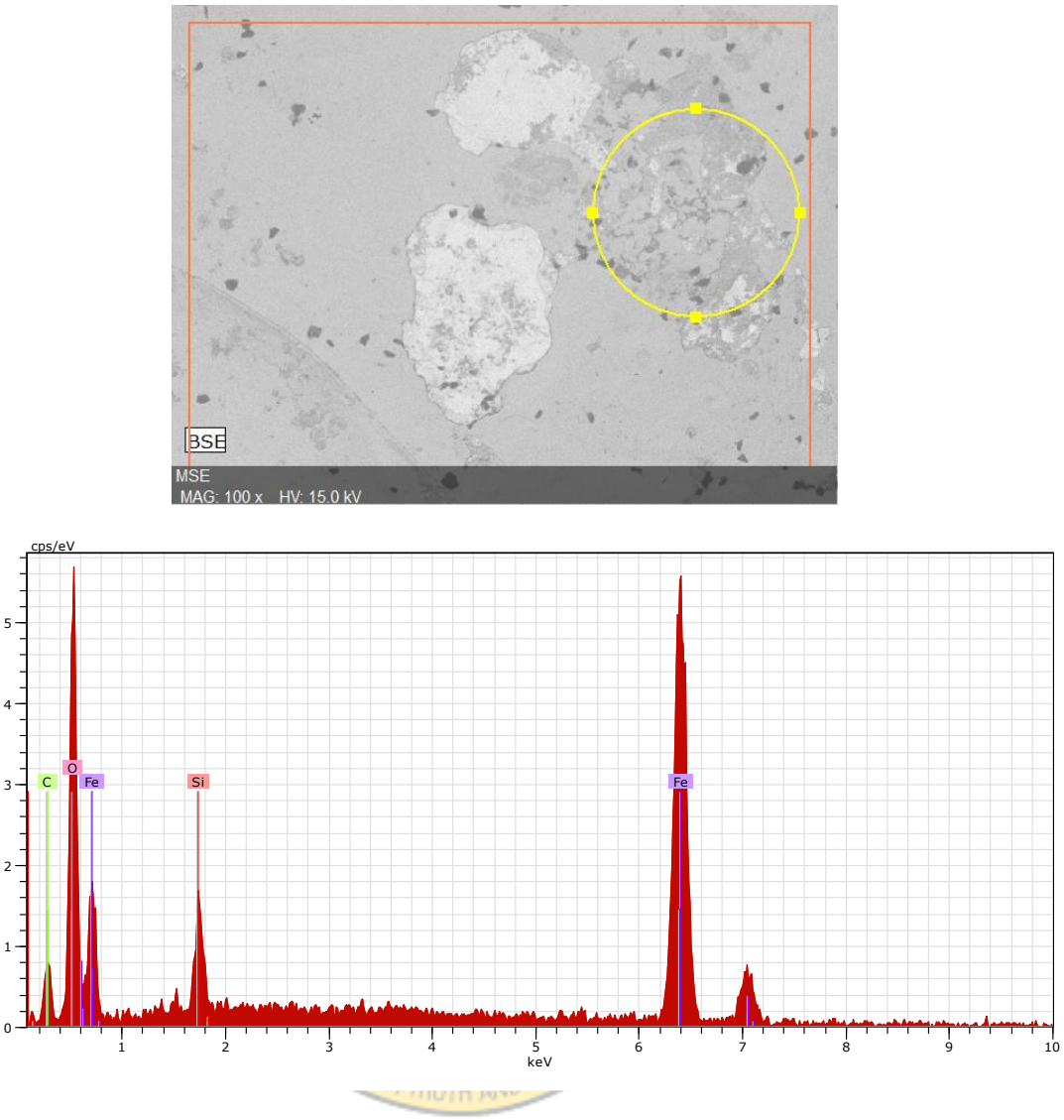

Figure 4.10 SEM/EDS Analysis of Reduced Iron Ore-ELT Composite Pellet (Region 4)

Table 4.5 Elemental Analysis of Region 4

Element	Mass %	Atom %
Fe	64.85	33.67
O	22.76	41.24
C	8.89	21.47
Si	3.50	3.62
Sum	100.00	100.00

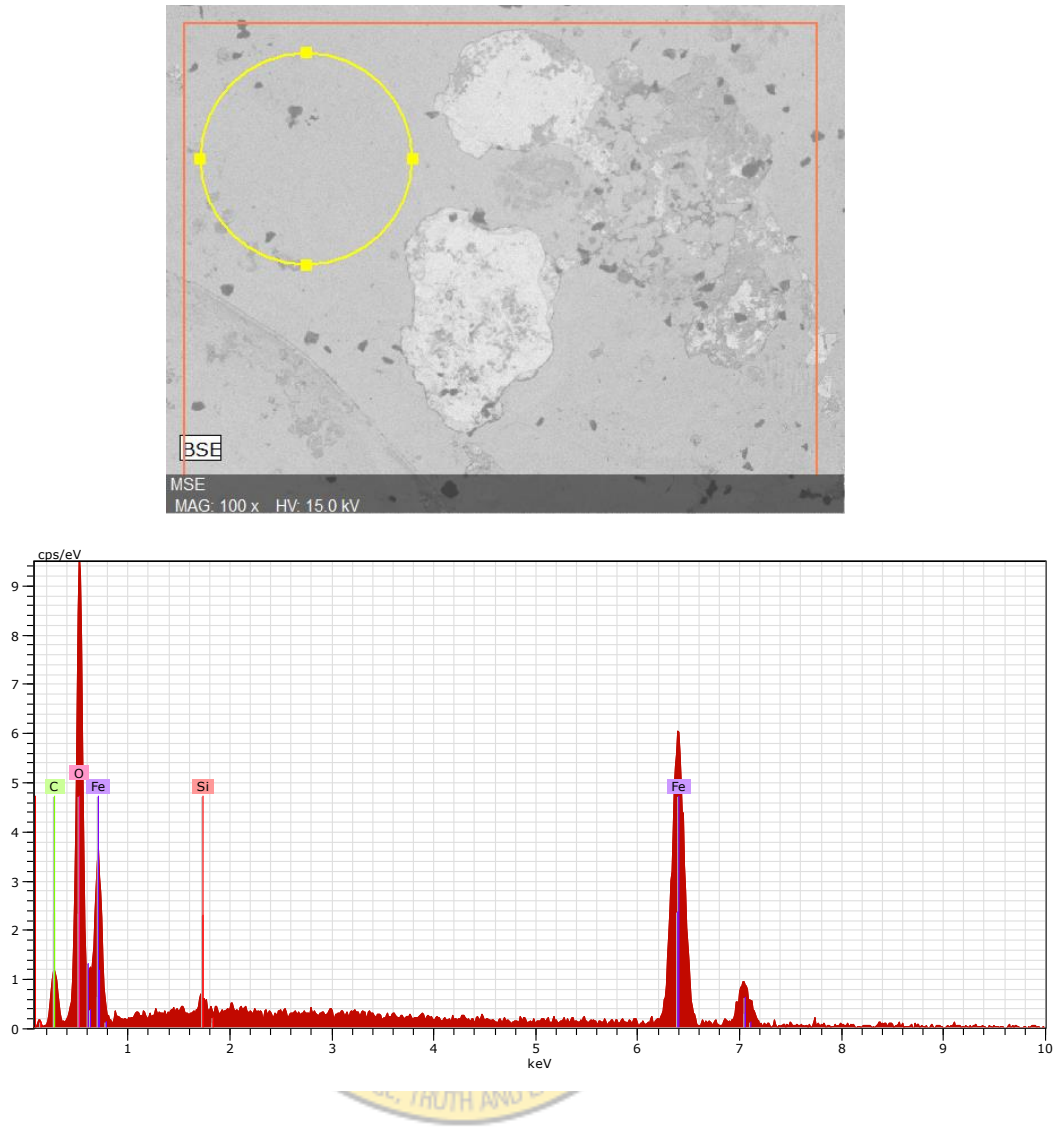

Figure 4.11 SEM/EDS Analysis of Reduced Iron Ore-ELT Composite Pellet (Region 5)

Table 4.6 Elemental Analysis of Region 5

Element	Mass %	Atom %
Fe	59.48	28.12
O	30.38	50.12
C	9.71	21.35
Si	0.44	0.41
Sum	100.00	100.00

The SEM-EDS results shows that at five different regions of the sample submitted, there is reduction of hematite to metal iron. The iron ore was reduced from 28.7% Fe to sponge iron with iron content ranging between 59% to 75% Fe. The carbon content was observed to range between 8.81% to 10.29%. This is an indication that carburization took place. The oxygen content is also in the range 14% to 30%.

4.2.4 Characterisation of Reduced Metal (Results of XRD Analyses)

The results of XRD analysis on the reduced pellets at 30, 40, 50 and 60 min. is given in Figures 4.12 to 4.15.

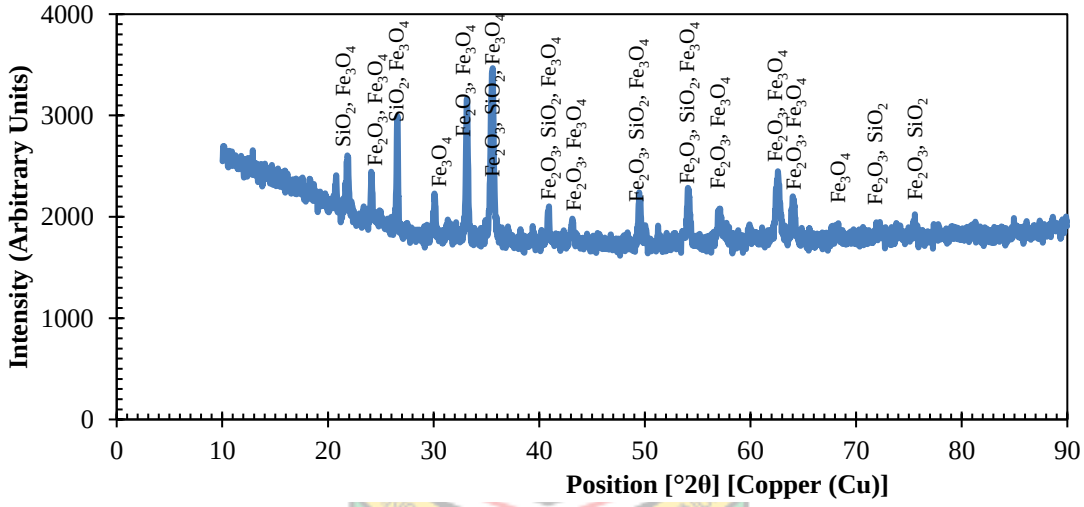

Figure 4.12 XRD of Reduced Iron Ore-ELT Composite Pellet at 30 minutes

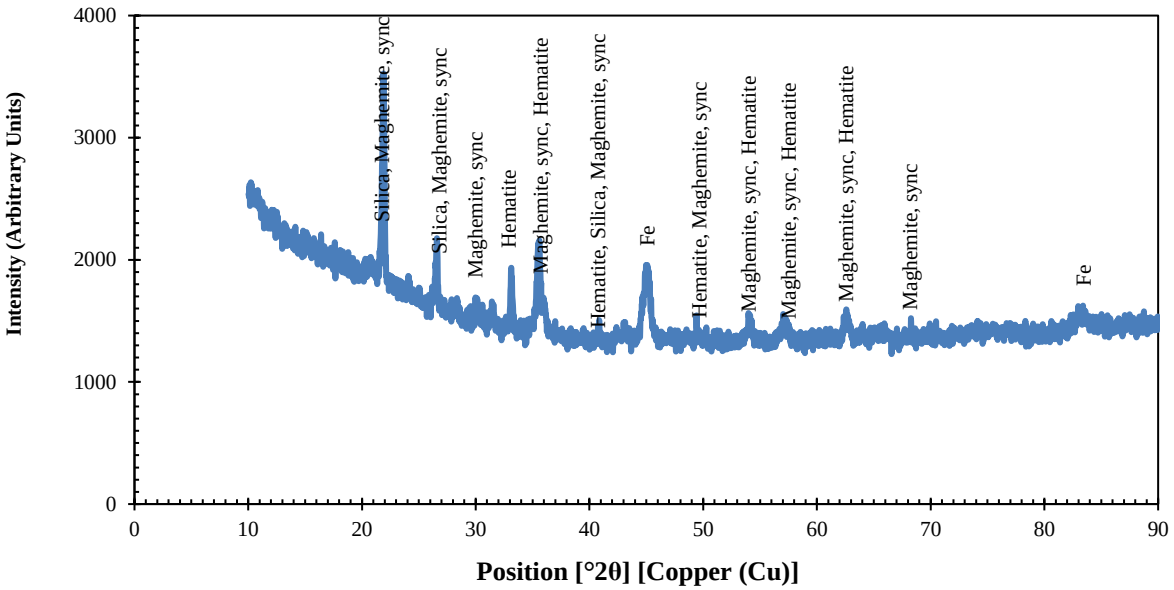

Figure 4.13 XRD of Reduced Iron Ore-ELT Composite Pellet at 40 minutes

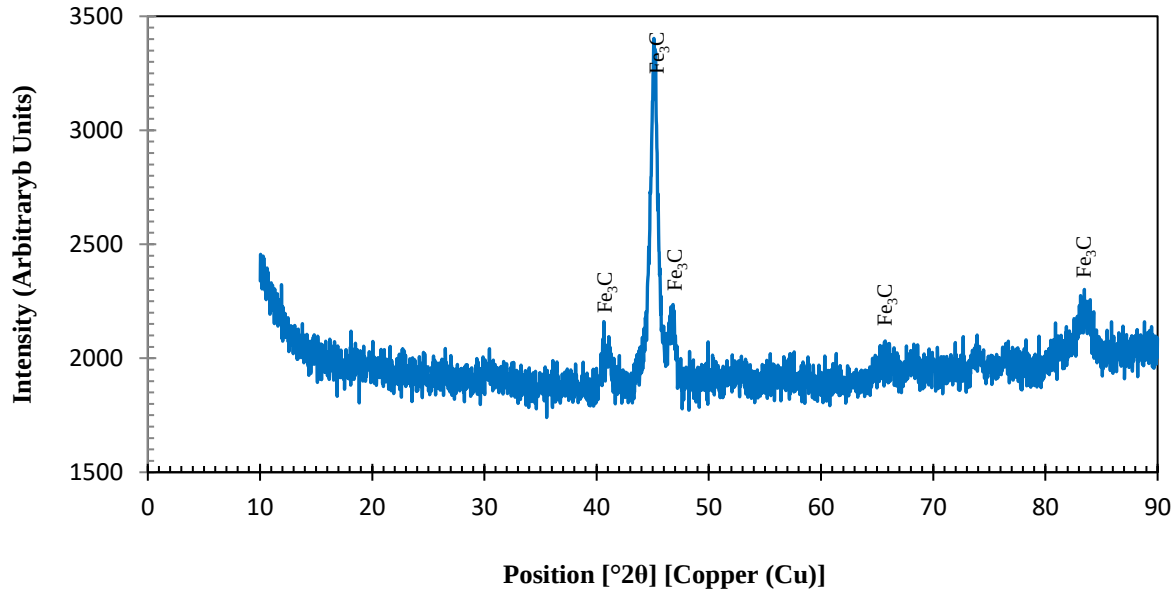

Figure 4.14 XRD of Reduced Iron Ore-ELT Composite Pellet at 50 minutes

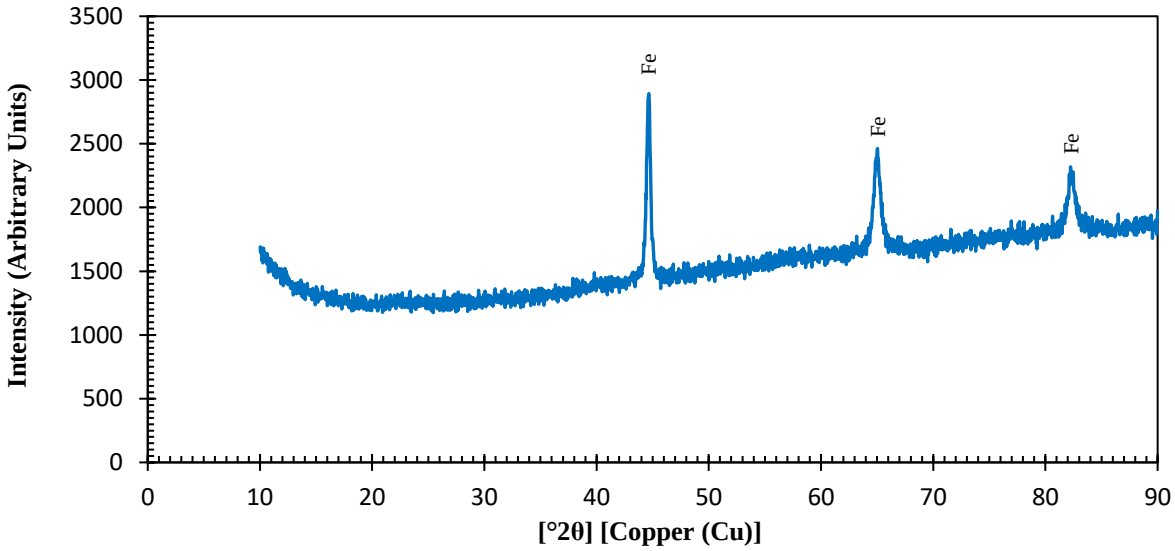

Figure 4.15 XRD of Reduced Iron Ore-ELT Composite Pellet at 60 minutes

In figure 4.12 and figure 4.13 it was observed that the reduced ore sample had some hematite, magnetite, silica and metal iron present. Figure 4.14 cementite was formed. In figure 4.15, hematite was reduced to metal iron. From the elemental analysis and XRD analysis, it is evident that reduction was complete at the end of the 60 mins. Since there was some greater degree of reduction from Fe_2O_3 to Fe, carbonaceous material in ELTs can be used as an alternative source of reductant for processing Opon Mansi iron ore.

4.2.5 Results of Gas Analysis during Reduction of Iron Ore-ELT Composite Pellet

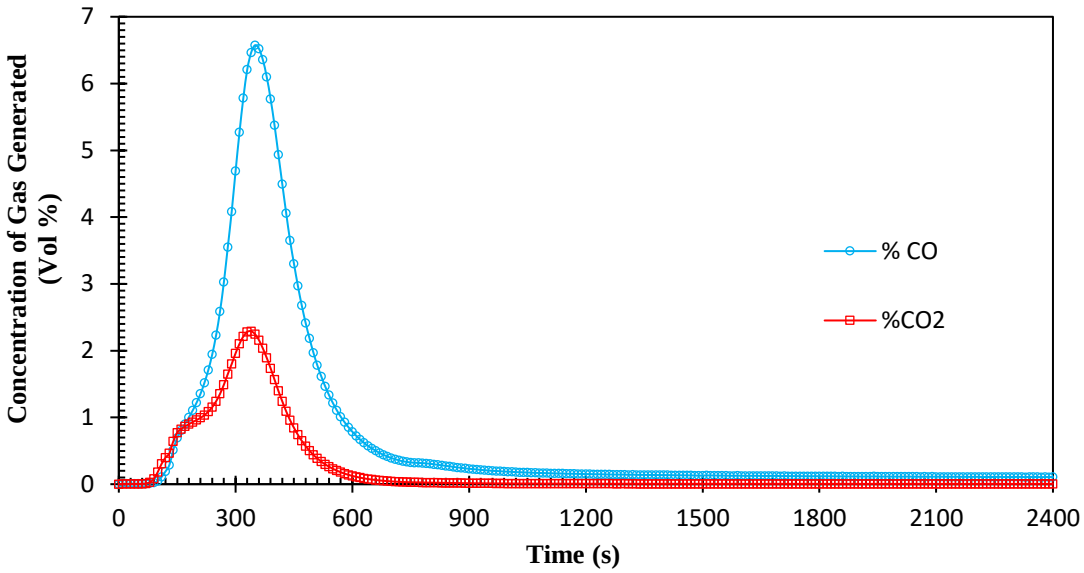

Figure 4.16 Concentrations of CO and CO_2 in the Off-Gas during Reduction of Iron Ore-ELT Composite Pellet at 1250 °C

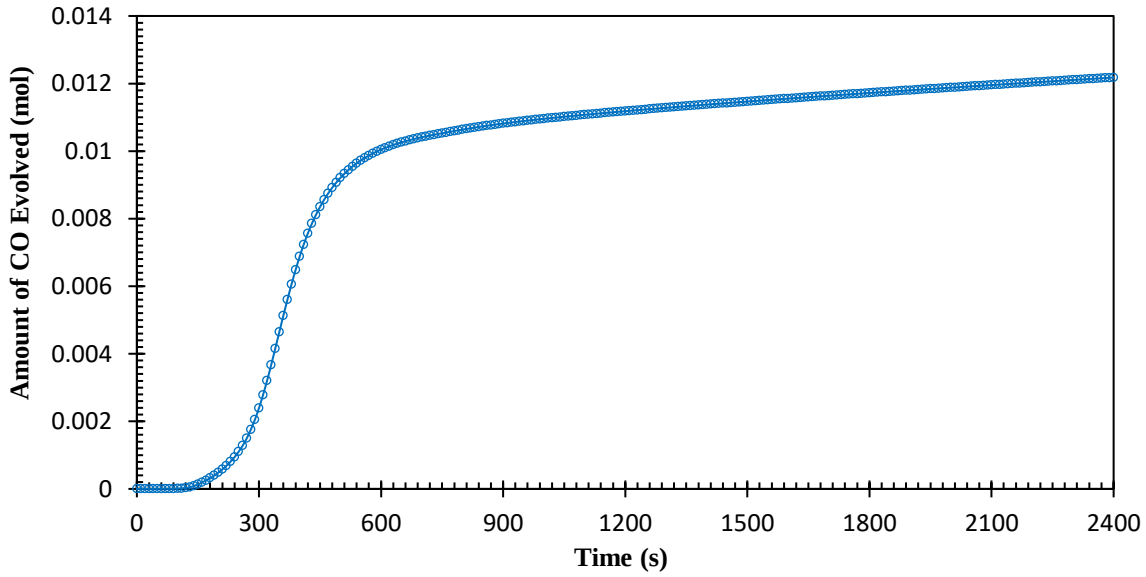

Figure 4.17 Amount of CO Generated during Reduction of Iron Ore-ELT Composite Pellet at 1250 °C

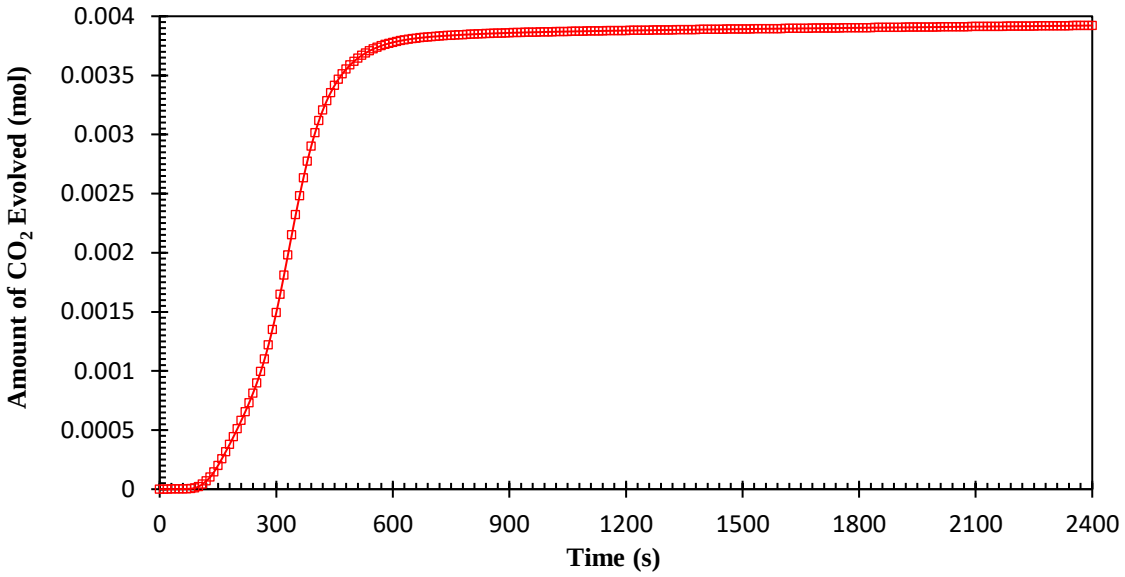

Figure 4.18 Amount of CO_2 Generated during Reduction of Iron Ore-ELT Composite Pellet at 1250 °C

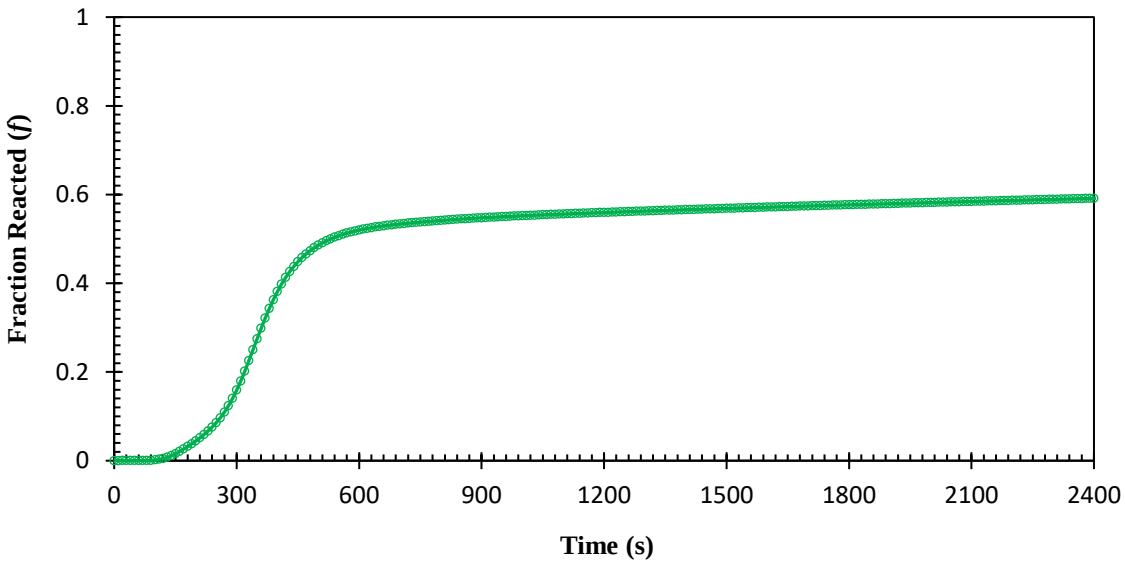

Figure 4.19 Fraction of Iron Ore-ELT Composite Pellet Reacted (f) as a Function of Time at 1250 °C

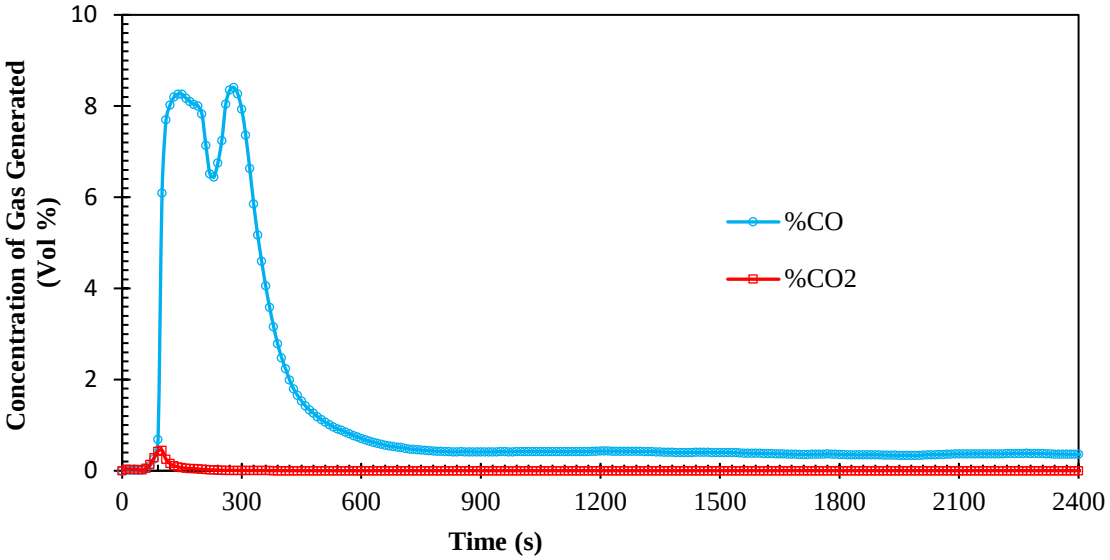

Figure 4.20 Concentrations of CO and CO_2 in the Off-Gas during Reduction of Iron Ore-ELT Composite Pellet at 1450 °C

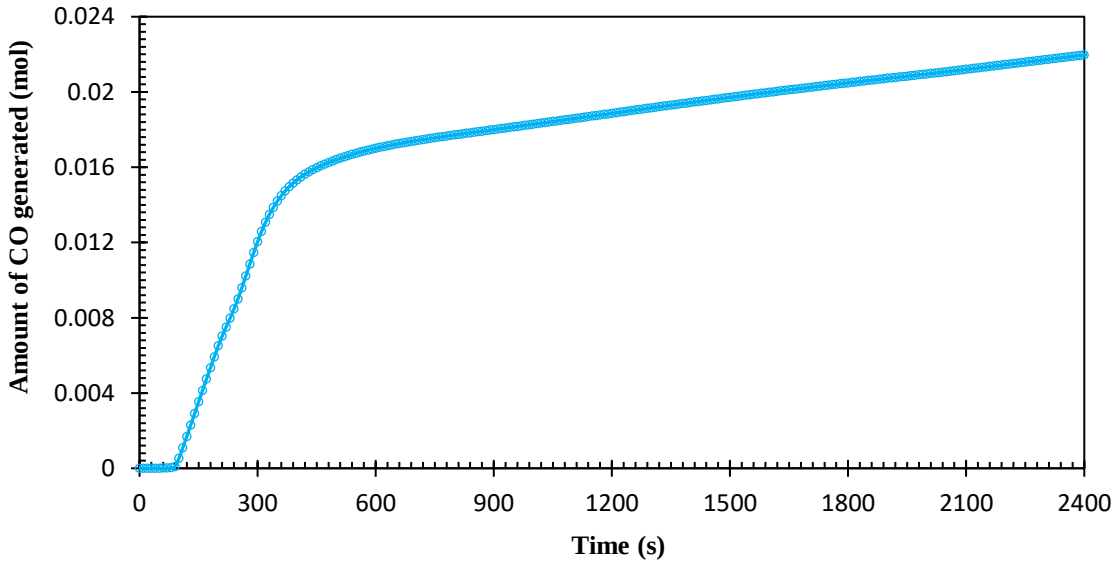

Figure 4.21 Amount of CO Generated during Reduction of Iron Ore-ELT Composite Pellet at 1450 °C

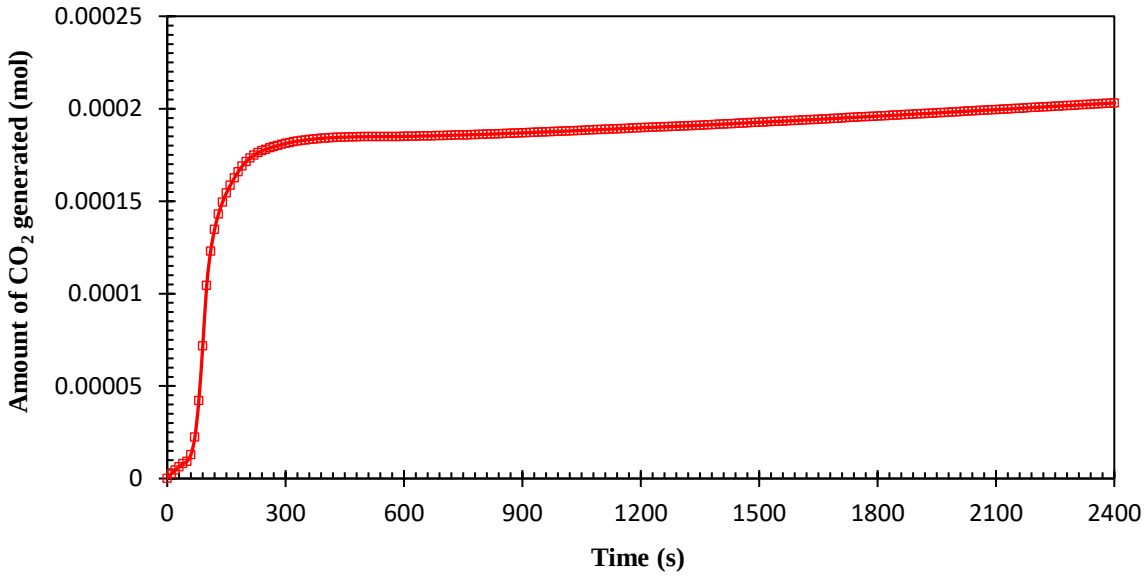

Figure 4.22 Amount of CO_2 Generated during Reduction of Iron Ore-ELT Composite Pellet at 1450 °C

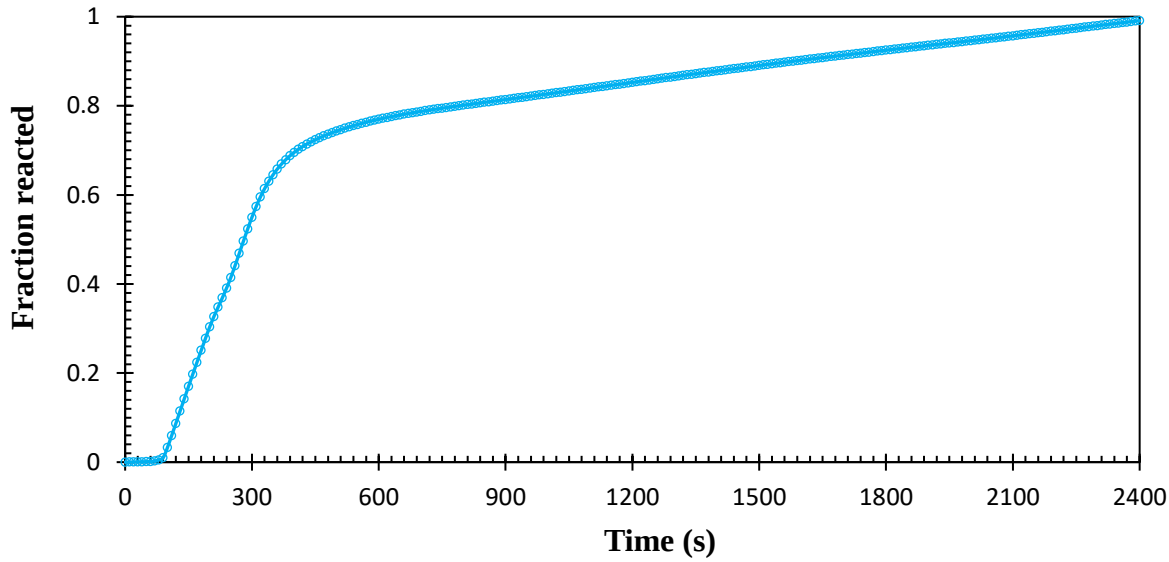

Figure 4.23 Fraction of Iron Ore-ELT Composite Pellet Reacted (f) as a Function of Time @ 1450 °C

The rate of CO removal from the pellet was calculated using the off-gas data. The results are shown in Figure 4.16 to figure 4.23. The Concentrations of CO and CO_2 in the off-gas during reduction of Iron Ore-ELT at 1250 ^oC attained its maximum peak at 360 seconds. The amount of CO generation for ELT became significant after 170 seconds, and then attained a maximum after 560 seconds.

When the iron ore-ELT was reduced at 1450 °C, a double peak concentration for CO was observed at 170 and 290 seconds. This is because at temperatures between 1400 ^oC and 1550 ^oC, the carburisation of silica occurs. This emits CO. The carburization reaction is shown in equation 4.1 below.

$$SiO_2 + 3C = SiC + 2CO \quad (4.1)$$

(Abolpour and Shamsoddini, 2019)

It was observed that CO emissions are higher than the corresponding CO_2 emissions. The relatively lower values recorded for CO_2 compared to CO may be an indication of direct reduction of Fe_2O_3 by C or a dominant Boudouard reaction or carbon gasification reaction (Dankwah *et al.*, 2011) .

The extent of reduction was determined from the calculated oxygen values along with the CO and CO_2 from the off-gas, having the knowledge that the initial concentration of removable oxygen from the reducible component of the iron ore is about 36.65%. The extent of reduction, f, was plotted as a function of time in figure 4.19 and figure 4.23. From figure 4.19 the extent of reduction progressed to 59% at a temperature of 1250 ^oC while in figure 4.23 the extent of reduction progressed steadily to 99% at a temperature of 1450 ^oC.

CHAPTER 5
CONCLUSIONS AND RECOMMENDATIONS

5.1 Conclusions

A laboratory investigation was conducted on the nature of Opon Mansi iron ore deposit and how it responds to reduction utilising End-of-Life Tyres (ELTs) as reducing agent. Based on the various test work carried out in these studies, the following are major findings from the studies:

a. The Opon Mansi iron ore is a low grade Hematite ore with an average grade of 41.07 wt% Fe_2O_3 (28.75 wt% Fe), with the presence of TiO_2 (1.26 wt%) and (0.03 wt%) sulphur.
b. ELTs are potential source of carbonaceous material for iron oxide reduction, since the extent of reduction from 100% Hematite to metal iron was 94.49%. The maximum iron content was also 75%Fe.
c. There was some degree of carburization of the reduced metal with 10% carbon.
d. There was not much impact when Pudo non magnetic flux was added, since the extent of reduction for the blend ranged between 77% and 94%.
e. The main gases that were present are CO and CO_2

5.2 Recommendations

From the studies conducted, the following rrecommendations were made;

a. Futher work should be conducted to pre-concentrate the low grade to a high grade feed to improve upon the iron recovery.
b. Charring of ELTs should be conducted in a fume chamber.
c. Futher work should be conducted to investigate the effect of particle size distribution on the reducibility of Opon Mansi iron ore.

REFERENCES

Abolpour, B., and Shamsoddini, R. (2019) "Mechanism of reaction of silica and carbon for producing silicon carbide", *Progress in Reaction Kinetics and Mechanism*, Vol. 45, pp. 1–14.

Abotar, E. (2019), "Studies the Nature of the Pudo Iron Ore and its Response to Reduction Using End-Of-Life Tyres", Unpublished MSc Thesis, University of Mines and Technology, 98pp.

Akhtar, K., Khan, S. A., Khan, S. B., and Asiri, A. M. (2018), "Scanning Electron Microscopy: Principle and Applications in Nanomaterials Characterization", In *Handbook of Materials Characterization*, pp. 113-145.

Amikiya, C. A. (2014), "*Characterisation of Iron Ore — A Case Study of Mount Tokadeh, Western Nimba Area, Liberia"*, *Unpublished MSc Thesis*, Kwame Nkrumah University of Science and Technology, 119pp.

Anameric, B., Rundman, K. B., and Kawatra, S. K. (2006), "Carburization Effects on Pig Iron Nugget Making", *Minerals and Metallurgical Processing*, Vol. *23*, No.3, pp. 139–150.

Anon. (2007). "Rubber Chemistry". *Matador Rubber s.r.o.,* 94pp.

Bahgat, M., Abdel Halim, K. S., El-Kelesh, H. A., and Nasr, M. I. (2012), "Blast Furnace Operating Conditions Manipulation for Reducing Coke Consumption and CO_2 Emission", *Steel Research International,* Vol. 83, No.7, pp. 686–694.

Béchara, R., Hamadeh, H., Mirgaux, O., and Patisson, F. (2020), "Carbon Impact Mitigation of the Iron Ore Direct Reduction Process Through Computer-Aided Optimization and Design Changes", *Metals*, Vol. 10, No. 3, pp. 1–12.

Bonilla-Cruz, J., Hernández-Mireles, B., Mendoza-Carrizales, R., Ramírez-Leal, L. A., Torres-Lubián, R., Valle, L. F. R., Paul, D. R., and Saldívar-Guerra, E. (2017),

"Chemical Modification of Butyl Rubber with Maleic Anhydride via Nitroxide Chemistry and its Application in Polymer Blends", *Polymers*, Vol. 9, No.2, 63pp.

Bunaciu, A. A., Udriştioiu, E. gabriela, and Aboul-Enein, H. Y. (2015), "X-Ray Diffraction: Instrumentation and Applications", *Critical Reviews in Analytical Chemistry*, Vol. 45, No.4, pp. 289–299.

Celikdemir, M., Sarikaya, M., Depci, T., Aydogmus, R., and Yucel, A. (2018), "Calcination and Pelletizing of Siderite Ore", *Iron Ore and Iron Oxide materials*, PP. 81-103.

Chanda, M. (2018), "*Plastics Technology Handbook*" , Taylor & Francis Group, LLC. Vol. 5, pp. 434-474.

Chauhan, A., and Chauhan, P. (2014), "Powder XRD Technique and its Applications in Science and Technology", *Journal of Analytical & Bioanalytical Techniques*, Vol. 5*,* No.5, 5pp.

Chen, Z. W., Gibson, W. M., and Huang, H. (2008), "High Definition X-Ray Fluorescence: Principles and Techniques", *X-Ray Optics and Instrumentation*, Vol. 2008, pp. 1–10.

Copeland, C.R., and Kawatra, S.K. (2005), "Dust suppression in iron ore processing plants", *Minerals & Metallurgical Processing*, Vol 22. No 4. Nov. pp 177-191.

Dankwah, J R. (2018), "Laboratory Studies on the Effect of End-of-Life Rubber Tyre Blending with Metallurgical Coke on Slag Foaming in Electric Arc Furnace Steelmaking", *Ghana Journal of Technology,* Vol. 3, No. 1, pp. 48–57.

Dankwah, J R, Yussif, I., Hinson, O. S., Owusu, C. K., Agorhom, E. A., Koshy, P., and Star, G. (2018), "Application of Microwave Technology to the Production of Iron Nuggets from the Sheini Iron Ore using Mixed Plastics Waste as Reductants", *Ghana Journal of Technology,* Vol. 2*,* No*.* 2, pp. 79–87.

Dankwah, J. R., Amoah, T., Dankwah, J., and Fosu, A. Y. (2015), "Recycling Mixed

Plastics Waste as Reductant in Ironmaking", *Ghana Mining Journal*, Vol. 15, No. 2, pp. 73 – 80.

Dankwah, J. R., and Koshy, P. (2013), "Production of Metallic Iron From Iron Oxide (Fe_2O_3) Using End-of-Life Rubber Tyre and its Blends with Metallurgical Coke as Reductants", *International Journal of Engineering Research in Africa*, Vol. 10 pp. 1-12.

Dankwah, J. R., Koshy, P., O'Kane, P., and Sahajwalla, V. (2012), "Reduction of FeO in EAF Steelmaking Slag by Blends of Metallurgical Coke and End-Of-Life Tyre", *Steel Research International*, Vol. *83*, No.8, pp. 766–774.

Dankwah, J. R., Koshy, P., Saha-Chaudhury, N. M., O'Kane, P., Skidmore, C., Knights, D. and Sahajwalla, V. (2011), "Reduction of FeO in EAF Steelmaking Slag by Blends+ of Metallurgical Coke and Waste Plastics", *ISIJ International*, Vol. 51, No. 3, pp. 498-507.

Dutta, S. K., and Chokshi, Y. B. (2020), "*Basic Concepts of Iron and Steel Making*", Springer Nature Singapore Pte Ltd, 645pp.

Dutta, S. K., and Sah, R. (2016), "Direct Reduced Iron: Production" *In Encyclopaedia of Iron, Steel, and Their Alloys,* Taylor and Francis: New York, Published online: *March 30*, pp. 1082–1108.

Evans, A., and Evans, R. (2006), "The Composition of a Tyre: Typical Components", *The Waste & Resources Action Programme,* 5pp.

Fernández-González, D., Piñuela-Noval, J., and Verdeja, L. F. (2018), "Iron Ore Agglomeration Technologies", *Iron Ores and Iron Oxide Materials*, . pp. 61-68.

Fragassa, C., and Ippoliti, M. (2016), "Technology Assessment of Tire Mould Cleaning Systems and Quality Finishing" *International Journal for Quality Research*, Vol. 10, No. 3, pp. 523–546.

Fru, E. C., Kilias, S., Ivarsson, M., Rattray, J. E., Gkika, K., McDonald, I., He, Q., and Broman, C. (2018), "Sedimentary Mechanisms of a Modern Banded Iron Formation on Milos Island, Greece", *Solid Earth*, Vol. 9, No. 3, pp. 573–598.

Girão, A. V., Caputo, G., and Ferro, M. C. (2017), "Application of Scanning Electron Microscopy–Energy Dispersive X-Ray Spectroscopy (SEM-EDS)", *Comprehensive Analytical Chemistry*, Vol. 75, pp. 153–168.

Gomes, O. F. M., and Paciornik, S. (2008), "Iron Ore Quantitative Characterisation Through Reflected Light-Scanning Electron Co-site Microscopy", *International Congress for Applied Mineralogy,* Vol. 9 , pp. 699–702.

Gupta, S., French, D., Sakurovs, R., Grigore, M., Sun, H., Cham, T., Hilding, T., Hallin, M., Lindblom, B., and Sahajwalla, V. (2008) "Minerals and iron-making reactions in blast furnaces", *Progress in Energy and Combustion Science*, Vol. 34, No. 2, pp. 155–197.

Habashi, F. (1997), "Handbook of Extractive Metallurgy", *Wiley-VCH*, Vol. 1, 488pp.

Hapugoda, S., Peterson, M. J., and Manuel, J. R. (2009), "Mineralogical and Textural Characterisation of Iron Ore from a Peruvian Magnetite-Haematite Skarn Prospect" *Iron Ore Conference*, Vol. 4, pp. 105–112.

Heikkilä, A., Iljana, M., Bartusch, H., and Fabritius, T. (2020), "Reduction of Iron Ore Pellets, Sinter, and Lump Ore under Simulated Blast Furnace Conditions", *Steel Research International*, Vol. 91, No. 11, 8pp.

Hesham, A. (2018), "New Trends in the Application of Carbon-Bearing Materials in Blast Furnace Iron-Making", *Minerals Mdpi*, Vol. 8, No. 12, pp. 1–20.

Hrstka, T., Gottlieb, P., Skála, R., Breiter, K., and Motl, D. (2018), "Automated Mineralogy and Petrology – Applications of TESCAN Integrated Mineral Analyzer (TIMA)", *Journal of Geosciences*, Vol. 63, No. 1, pp. 47–63.

Ishola, F. A., Ajayi, O. O., Oyawale, F. A., and Akinlabi, S. A. (2018), "Sustainable

End-of-Life tyre (EOLT) Management for Developing Countries - A review", *Proceedings of the International Conference on Industrial Engineering and Operations Management*, Vol. 1, pp. 1054–1064.

Kay, A. (2018), "Types of Iron Ore: Hematite vs. Magnetite", www.investingnews.com/daily/resource-investing/base-metals-investing/iron-investing/types-of-iron-ore-hematite-vs-magnetite, Accessed July 20, 2020

King, M.H. (2020), "Limonite", www.geology.com/minerals/limonite.shtml , Accessed August 15, 2020

Kiptarus, J. J., Muumbo, A. M., Makokha, A. B., and Kimutai, S. K. (2015), "Characterization of Selected Mineral Ores in the Eastern Zone of Kenya: Case Study of Mwingi North Constituency in Kitui County", *International Journal of Mining Engineering and Mineral Processing*, Vol. 4 No.1, pp. 8–17.

Kolawole, O. J., Akanni, A. A., Ameenullahi, B. S., and Adediran, A. A. (2019), "Preliminary Characterisation ofIiron Ores for Steel Making Processes", *Proceeding of 2nd International Conference on Sustainable Materials Processing and Manufacturing*, Vol. 35, pp. 1123–1128.

Koleini, S. M. J., and Barani, K. (2012), "Microwave Heating Applications in Mineral Processing", *The Development and Application of Microwave Heating*, published online: November 7, 2012, pp. 79-104.

Kondrin, M. V., Lebed, Y. B., and Brazhkin, V. V. (2016), "Structure and Topology of Three-Dimensional Hydrocarbon Polymers", *Acta Crystallographica Section B: Structural Science, Crystal Engineering and Materials*, Vol. 72, No. 4, pp. 634–641.

Krieger, B., and Tredinnick, D. W. (2002), "Industrial Microwave Teachnology", *Proceedings at Annual Meeting of the Rubber Division of the American Chemical Society Conference*, Vol. 4, 22pp.

Krishna, S. J. G., Patil, M. R., Rudrappa, C., Kumar, S. P., and Ravi, B. P. (2013), "Characterisation and Processing of Some Iron Ores of India", *Journal of The Institution of Engineers*, Vol. 94, No. 2, pp. 113–120.

Kumar, V., Jadhav, G. N., Khosla, N. K., Chattoraj, U. S., R.P. Bhagat, Singh, R., Nayak, B., Mohanta, M. K., Bhattacharyya, K. K., and Mehrotra, S. P. (2007), "Characterization and its Implication on Beneficiation of Low Grade Iron Ore By Gravity Separation", *Advanced Gravity Separation*, , pp. 10–23.

Landi, D., Vitali, S., and Germani, M. (2016), "Environmental Analysis of Different End of Life Scenarios of Tires Textile Fibers", *Procedia CIRP*, Vol. 48, pp. 508–513.

Lascelles, D. F. (2012), "Banded iron formation to high-grade iron ore: A critical review of supergene enrichment models", *Australian Journal of Earth Sciences*, Vol. 59, No. 8, pp 1105–1125.

Lavina, B., Dera, P., and Downs, R. T. (2014), "Modern X-ray diffraction methods in mineralogy and geosciences", *Reviews in Mineralogy and Geochemistry*, Vol. 78, pp. 1–31.

Lim, C. H., and Sirisomboon, P. (2017), "Evaluation of prevulcanisate relaxed modulus of prevulcanised natural rubber latex using Fourier transform near infrared spectroscopy", *Journal of Near Infrared Spectroscopy*, Vol. 25, No. 6, pp. 407-415.

Lu, L., Holmes, R. J., and Manuel, J. R. (2007), "Effects of alumina on sintering performance of hematite iron ores", *ISIJ International*, Vol. 47 No. 3, pp. 349–358.

Lu, Liming. (2015), "Iron ore: Mineralogy, processing and environmental sustainability". *Elsevier Science, 666pp.*

Lundgren, M. (2010), "Blast Furnace Coke Properties and the Influence on Off-gas Dust", *Licenciate Thesis*. Luleå University of Technology, 54pp

Michaud, D. (2016), "Different Types of Iron Ore",*Www.911metrallurgist.Com/Blog/Different-Types-Iron-Ore*, Accessed: August 20, 2020.

Moraes, S. L. de, Lima, J. R. B. de, and Ribeiro, T. R. (2018), "Iron Ore Pelletizing Process: An Overview",*Iron Ores and Iron Oxide Materials,* pp. 42–59.

Muwanguzi, A. J. B., Karasev, A. V., Byaruhanga, J. K., and Jönsson, P. G. (2012a), "Characterisation of the Physical and Metallurgical Properties of Natural Iron Ore for Iron Production", *ISRN Materials Science*, Vol. 2012, 9pp.

Muwanguzi, A. J. B., Karasev, A. V., Byaruhanga, J. K., and Jönsson, P. G. (2012b), "Characterization of Chemical Composition and Microstructure of Natural Iron Ore from Muko Deposits", *ISRN Materials Science*, Vol. 2012, 9pp.

Ofoegbu, S. U. (2019), "Characterization studies on Agbaja iron ore: a high-phosphorus content ore", *SN Applied Sciences*, Vol. 1, No. 3, pp. 1–11.

Okeke, C., Abioye, A. E. B., and Omosun, Y. (2005), "Microwave heating in food processing", *IOSR Journal of Electrical and Electronics Engineering (IOSR-JEEE)*, Vol. 9, No. 4, pp. 2258–2272.

Okoro, F. E., Femi-Oyewole, D., Onkunlola, O., Antwi, A. A., and Ngassam, N. Y. (2017), "Technical and Economic Overview of Iron Ore Production in Australia", *Technical Report*, 15pp.

Oyedotun, T. D. T. (2018) "X-ray fluorescence (XRF) in the investigation of the composition of earth materials: a review and an overview", *Geology, Ecology, and Landscapes*, Vol. 2, No. 2, pp. 148–154.

Palacios, L. D. L. T. D. (2011), "Natural Resources Sustainability : Iron Ore Mining", *DYNA*, Vol. 78, No. 170, pp. 227–234.

Panias, D., and Krestou, A. (2004), "Use of microwave energy in metallurgy", *Proceedings on 1st International Conference on Advances in Mineral Resources Management and Environmental Geotechnology,* pp. 215–220.

Patra, S., and Rayasam, V. (2018), "Pelletization of iron ore fines with parameter optimization through box-behnken design", *Material Science & Engineering International Journal Research*, Vol. 2, No. 6, pp. 287–292.

Ramirez-Canon, A., Muñoz-Camelo, Y. F., and Singh, P. (2018), "Decomposition of used tyre rubber by pyrolysis: Enhancement of the physical properties of the liquid fraction using a hydrogen stream", *Environments - MDPI*, Vol. 5, No.6, pp. 1–12.

Ramos, G., Alguacil, F. J., and López, F. A. (2011), "The recycling of end-of-life tyres. Technological review", *Revista de Metalurgia*, Vol. 47, No.3, pp. 273–284.

Rao, D. S., Kumar, T. V. V., Rao, S. S., Prabhakar, S., and Raju, G. B. (2009), "Mineralogy and Geochemistry of A Low Grade Iron Ore Sample from Bellary-Hospet Sector , India and Their Implications on Beneficiation", *Journal of Minerals & Materials Characterization & Engineering,* Vol. 8, No. 2, pp. 115–131.

Sahajwalla, V., Zaharia, M., Rahman, M., Khanna, R., Saha-Chaudhury, N., O'Kane, P., Dicker, J., Skidmore, C., and Knights, D. (2011), "Recycling rubber tyres and waste plastics in EAF steelmaking", *Steel Research International*, Vol. 82, No. 5, pp. 566–572.

Satyananda, P., Kumar, A. and Rayasam, V. (2017) "The effect of particle size on green pellet properties of iron ore fines", *Journal of Mining and Metallurgy A: Mining*, Vol. 53, No. 1, pp. 31–41.

Satyendra, K. S. (2014a), "Beneficiation of Lateritic Iron Ores", *Www.Ispatguru.Com*, Accessed: August 28,2020.

Satyendra, K. S. (2014b), "Mining of iron ores", *Www.Ispatguru.Com*, Accessed:

August 19, 2020.

Schneider, J. M., Timken, C., and Chatterjee, S. M. (2013), "Steel Heat TreatingFundamentals and Processes". In *ASM Handbook,* Vol. 4A. pp. 390-398

Shahrampour, H. (2018), "Comparison of Sulfur Curing Systems (Insoluble-Rhombic) on Physical and Thermal Properties of the Matrix Polymeric of Styrene-Butadiene Rubber and Natural Rubber", *Petroleum Chemistry*, Vol. 58, No. 8, pp. 721–726.

Singh, G. P., Sundeep, Choudhary, R. P., Vardhan, H., Aruna, M., and Akolkar, A. B. (2015), "Iron Ore Pelletization Technology and its Environmental Impact Assessment in Eastern Region of India – A Case Study", *Procedia Earth and Planetary Science*, Vol. 11, pp. 582–597.

Smith, A. J. B., and Beukes, N. J. (2016), "Palaeoproterozoic banded iron formationhosted high-grade hematite iron ore deposits of the Transvaal Supergroup, South Africa", *Episodes*, Vol. 39, No. 2, pp. 269–284.

Standish, N., and Huang, W. (1991), "Microwave Application in Carbothermic Reduction of Iron Ores", *ISIJ International*, Vol. 31, No. 3, pp. 241–245.

Sun, S. (1997), "A Study of Kinetics and Mechanisms of Iron Ore Reduction in Oreicoal Composites". *PhD Thesis*, McMaster University , Canada, 198pp.

Suopajärvi, H., Kemppainen, A., Haapakangas, J., and Fabritius, T. (2017), "Extensive review of the opportunities to use biomass-based fuels in iron and steelmaking processes", *Journal of Cleaner Production*, Vol. 148, pp. 709–734.

Taylor, C. D., Schulz, K. J., Doebrich, J. L., Orris, G. J., Denning, P. D., and Kirschbaum, M. J. (2009), "Geology and Nonfuel Mineral Deposits of Africa and the Middle East", *U.S. Geological Survey Open-File Report 2005-1294-E*, 246pp.

Timbillah, S., Aabulleh, P. N., and Agorhom, E. A. (2007), "Iron ore surge in the world - The role of Ghana", *Proceedings of Iron Ore Conference*, August 20-22, pp. 197–202.

US EPA. (1994), "Extraction and beneficiation of ores and minerals"*, Technical Resource document*. Vol. 3, 122 pp.

Yang, H., Lu, R., Downs, R. T., and Costin, G. (2006), "Goethite, α -FeO(OH), from single-crystal data", *Acta Crystallographica Section E*, pp. 250–252.

Yerly, R. (2014), "XRF Technology for Non-Scientists", *Thermo Fisher Scientific*, 41pp.

Zaharia, M., Sahajwalla, V., Saha-Chaudhury, N., O'Kane, P., Fontana, A., Skidmore, C., and Knights, D. (2012), "Recycling of rubber tyres in electric arc furnace steelmaking: Carbon/slag reactions of coke/rubber blends", *High Temperature Materials and Processes*, Vol. 31, No. 4–5, pp. 593–602.

APPENDICES

Appendix A Reduction Analysis for Opon Mansi Iron Ore without Pudo flux

C 1						
DURATION	**BLENDS**	**Ore**	**MASS BEFORE REDUCTION(g)**	**MASS AFTER REDUCTION(g)**	**WEIGHT LOSS(g)**	**PERCENT REDUCTION(%)**
C20 min	100	**Oppong Mansi**	26.00	18.40	7.60	53.33
C30 miin	100		28.00	18.70	9.30	60.60
C40 min	100		29.30	13.20	16.10	100.25
C50 min	100		29.10	18.00	11.10	69.59
C60 min	100		29.00	13.50	15.50	97.52
C 2						
DURATION	**BLENDS**	**Ore**	**MASS BEFORE REDUCTION(g)**	**MASS AFTER REDUCTION(g)**	**WEIGHT LOSS(g)**	**PERCENT REDUCTION(%)**
C20 min	100	**Oppong Mansi**	29.70	13.70	16.00	98.29
C30 miin	100		25.00	16.70	8.30	60.57
C40 min	100		29.80	19.60	10.20	62.45
C50 min	100		30.20	21.50	8.70	52.56
C60 min	100		28.30	12.00	16.30	105.09

Appendix A Continued

C 3						
DURATION	**BLENDS**	**Ore**	**MASS BEFORE REDUCTION(g)**	**MASS AFTER REDUCTION(g)**	**WEIGHT LOSS(g)**	**PERCENT REDUCTION(%)**
C20 min	100	**Oppong Mansi**	30.50	17.70	12.80	76.57
C30 miin	100		29.80	21.30	8.50	52.04
C40 min	100		29.80	16.10	13.70	83.88
C50 min	100		30.00	19.60	10.40	63.25
C60 min	100		29.40	16.30	13.10	81.30
AVERAGE						
DURATION	**BLENDS**	**Ore**	**MASS BEFORE REDUCTION(g)**	**MASS AFTER REDUCTION(g)**	**WEIGHT LOSS(g)**	**PERCENT REDUCTION(%)**
C20 min	100	**Oppong Mansi**	28.73	16.60	12.13	77.04
C30 miin	100		27.60	18.90	8.70	57.51
C40 min	100		29.63	16.30	13.33	82.09
C50 min	100		29.77	19.70	10.07	61.70
C60 min	100		28.90	13.93	14.97	94.49

Appendix A continued

DURATION	AVERAGE PERCENT REDUCTION
20 min	77.04
30 min	57.51
40 min	82.09
50 min	61.70
60 min	94.49

Appendix B Reduction Anaysis for Opon Mansi Iron Ore with Pudo Flux

Part 2		Ore C 1			
Blends (%)		Intial Weight (g)	Final Weight (g)	Weight Loss (g)	Percent Reduction (%)
Oppong Mansi	Pudo Flux				
90	10	26.00	16.80	9.20	64.56
85	15	28.10	15.20	12.90	83.76
80	20	28.30	8.80	19.50	125.72
75	25	27.50	14.50	13.00	86.25
70	30	27.20	11.70	15.50	103.97
60	40	28.80	15.60	13.20	83.62
50	50	28.00	17.20	10.80	70.37
Ore C 2					
Blends (%)		Intial Weight (g)	Final Weight (g)	Weight Loss (g)	Percent Reduction (%)
Oppong Mansi	Pudo Flux				
90	10	23.60	12.90	10.70	82.72
85	15	26.50	13.30	13.20	90.88
80	20	27.20	15.30	11.90	79.82
75	25	27.10	16.60	10.50	70.69
70	30	28.50	15.30	13.20	84.50
60	40	27.50	15.80	11.70	77.62
50	50	28.80	14.30	14.50	91.86

Appendix B Continued

Ore C 3					
Blends (%)		**Intial Weight (g)**	**Final Weight (g)**	**Weight Loss (g)**	**Percent Reduction (%)**
Oppong Mansi	**Pudo Flux**				
90	10	24.10	12.80	11.30	85.55
85	15	27.80	14.80	13.00	85.32
80	20	26.00	15.30	10.70	75.08
75	25	27.00	15.70	11.30	76.36
70	30	30.20	17.30	12.90	77.93
60	40	30.20	12.80	17.40	105.12
50	50	30.30	16.80	13.50	81.29
Average					
Blends (%)		**Intial Weight (g)**	**Final Weight (g)**	**Weight Loss (g)**	**Percent Reduction (%)**
Oppong Mansi	**Pudo Flux**				
100	0	28.90	13.93	14.97	94.49
90	10	24.57	14.17	10.40	77.24
85	15	27.47	14.43	13.03	86.57
80	20	27.17	13.13	14.03	94.25
75	25	27.20	15.60	11.60	77.81
70	30	28.63	14.77	13.87	88.36
60	40	28.83	14.73	14.10	89.22
50	50	29.03	16.10	12.93	81.27

Appendix B Continued

SAMPLE	OPON MANSI(%)	PUDO FLUX (%)	AVERAGE PERCENT REDUCTION
C60min	100	0	94.49
A	90	10	77.24
B	85	15	86.57
C	80	20	94.25
D	75	25	77.81
E	70	30	88.36
F	60	40	89.22
G	50	50	81.27

INDEX

B

C

F

G

M

N

O

P

Q

R

S

T

U

V

W

X